Leishmania major degrades murine CXCL1 – an immune evasion strategy

Matthew S. Yorek[1,2], Barun Poudel[1,2], Lalita Mazgaeen[1,2,4], R. Marshall Pope[5], Mary E. Wilson[2,3,6,7,8], Prajwal Gurung[1,2,3,4,*]

[1] Inflammation Program, University of Iowa, Iowa City, IA, USA
[2] Department of Internal Medicine, University of Iowa, Iowa City, IA, USA
[3] Immunology Graduate Program, University of Iowa, Iowa City, IA, USA
[4] Interdisciplinary Graduate Program in Human Toxicology, University of Iowa, Iowa City, IA, USA
[5]The Proteomics Facility, University of Iowa, Iowa City, IA, USA.
[6]Department of Microbiology and Immunology, University of Iowa, Iowa City, IA, USA
[7]Department of Epidemiology, University of Iowa, Iowa City, IA, USA
[8]Iowa City VA Medical Center, Iowa City, IA, USA

***Correspondence should be addressed to:**
Prajwal Gurung
Inflammation Program, Department of Internal Medicine
University of Iowa
431 Newton Road, 429 EMRB
Iowa City, IA 52242
Tel: (319) 335-4536; Fax: (319) 335-4194
E-mail: prajwal-gurung@uiowa.edu

Running title: *Leishmania spp.* degrades CXCL1

Keywords: Leishmania, CXCL1, leishmaniasis, metalloprotease

Summary sentence: *L. major* metalloproteases can specifically degrade murine CXCL1 to subvert the host immune response and establish infection.

Abstract

Leishmaniasis is a global health problem with an estimated report of 2 million new cases every year and more than 1 billion people at risk of contracting this disease in endemic areas. The innate immune system plays a central role in controlling *L. major* infection by initiating a signaling cascade that results in production of pro-inflammatory cytokines and recruitment of both innate and adaptive immune cells. Upon infection with *L. major*, CXCL1 is produced locally and plays an important role in the recruitment of neutrophils to the site of infection. Herein, we report that *L. major* specifically targets murine CXCL1 for degradation. The degradation of CXCL1 is not dependent on host factors as *L. major* can directly degrade recombinant CXCL1 in a cell-free system. Using mass spectrometry, we discovered that the *L. major* protease cleaves at the C-terminal end of murine CXCL1. Finally, our data suggest that *L. major* metalloproteases are involved in the direct cleavage and degradation of CXCL1, and a synthetic peptide spanning the CXCL1 cleavage site can be used to inhibit *L. major* metalloprotease activity. In conclusion, our study has identified an immune evasion strategy employed by *L. major* to evade innate immune responses in mice, likely reservoirs in the endemic areas, and further highlights that targeting these *L. major* metalloproteases may be important in controlling infection within the reservoir population and transmittance of the disease.

Authors' summary

Our study discovered a highly specific role for *L. major* metalloprotease in cleaving and degrading murine CXCL1. Indeed, *L. major* metalloprotease did not cleave murine CXCL2 or human CXCL1, CXCL2 and CXCL8. CXCL1 is a critical chemokine required for neutrophil recruitment to the site of infection; thus, we propose that this metalloprotease may have evolved to evade immune responses specifically in the murine host. We have further identified that the C-terminal end on CXCL1 is targeted for cleavage by the *L. major* metalloprotease. Finally, this cleavage site information was used to design peptides that are able to inhibit CXCL1 degradation by *L. major*. Our study highlights an immune evasion strategy utilized by *L. major* to establish infection within a murine host.

61 **Introduction**

62 *Leishmania spp.* are unicellular eukaryotic protozoan parasites that are transmitted to
63 mammalian hosts by sandfly (*Phlebotomine and Lutzomyia spp.*) bites [1]. Upon
64 transmission of *L. major* promastigotes (the infectious stage for mammalian hosts with a
65 long slender body and an anterior flagellin), the promastigotes are quickly taken up by
66 neutrophils, macrophages and keratinocytes [2-6]. Within the macrophages, *Leishmania*
67 *spp.* promastigotes hijack the phagocytic vacuole and transform into amastigotes (round
68 body lacking an anterior flagellin) [7]. The *Leishmania spp.* amastigotes then proliferate
69 within the vacuole and establish infection within the host [8, 9]. While a mammalian
70 host-vector system is the major mode of *Leishmania spp.* transmission, several studies
71 have reported a vertical transmission of these parasites in mammalian hosts, from a
72 pregnant female to its offspring [10-13]. Specifically, *Leishmania spp.* infection has been
73 found to be endemic in foxhound dog populations in the United States, where the
74 vectors are not present [14-17]. Given that *Leishmania spp.* can infect several hosts,
75 including rodents and dogs (in addition to humans) [18], these studies demonstrate how
76 these parasites can remain endemic even with strategies to eradicate sandflies.
77

78 Our immune system is extremely efficient in killing pathogens. Professional phagocytes
79 such as macrophages and neutrophils phagocytose and kill the invading pathogen in
80 the intracellular phagosome-lysosome compartment. In addition, these phagocytes also
81 respond to the foreign pathogens by secreting pro-inflammatory cytokines and
82 chemokines to recruit neutrophils to the site of infection [19-21]. *Leishmania spp*. have
83 evolved to evade the host immune response by using its armada of virulence factors to

84 avoid host killing [22]. The two major virulence factors of *Leishmania spp.* include
85 leishmanolysin metalloprotease glycoprotein 63 (GP63) and lipophosphoglycan (LPG),
86 and both have been extensively studied for their roles in immune evasion [23, 24].
87 GP63 and LPG inhibit the formation of the membrane attack complex to evade
88 complement-mediated lysis [25, 26], inhibit acidification of leishmania containing
89 vacuoles [27, 28], and dampen host immune signaling pathways [29, 30] for
90 establishing infection within the mammalian host. In addition, *Leishmania spp.* can
91 hijack the host immune responses to establish infections as shown by *Leishmania*
92 *chagasi (L. chagasi)*-mediated activation of TGF-β and *Leishmania major (L. major)*-
93 induced activation of NLRP3 inflammasome, events that promote *L. major* survival and
94 pathology [31-33]. Here, we have identified one such immune evasion mechanism
95 employed by *L. major*.
96
97 *L. major* is the most common *Leishmania spp.* and a major cause of cutaneous
98 leishmaniasis that affects 600,000-1,000,000 people globally [34]. Once deposited at
99 the site of a sandfly bite, *L. major* promastigotes are taken up by the resident
100 macrophages and keratinocytes, which then secrete essential cytokines and
101 chemokines to elicit an innate immune response [35]. One of the earliest chemokines
102 that are produced in the skin in response to *L. major* include CXCL1 [36]. CXCL1 is a
103 functional homolog of human IL-8 in mice and a potent neutrophil chemoattractant [37-
104 41]. Keratinocytes [3], neutrophils [42] and macrophages [43, 44] have all been
105 suggested to produce CXCL1 (or IL-8 in humans) in response to *Leishmania spp.*
106 infection. Several studies have shown that neutrophils infiltrate the site of *Leishmania*

107 *spp.* infection as early as 1-hour post-infection and are important for optimal resolution
108 of the infection [21, 45]. Given the importance of CXCL1 in modulating the early innate
109 immune response, we reasoned that *L. major* targets CXCL1 to evade early host innate
110 immune responses.
111
112 In this current study, we have identified murine CXCL1 as a highly specific substrate for
113 *L. major* metalloprotease and a possible immune evasion strategy employed by this
114 parasite to establish a successful infection within the murine host. We further report that
115 *L. major* promotes proteolytic cleavage of murine CXCL1 at the C-terminal end to
116 initiate its degradation. Finally, we have designed a synthetic peptide spanning the
117 CXCL1 cleavage site that inhibits *L. major* protease activity. In conclusion, our study
118 has uncovered a specific mechanism employed by *L. major* to degrade murine CXCL1
119 which may help the parasite to establish infection within the murine host.
120
121

122 **Results**

123 ***L. major* infection abrogates LPS-induced CXCL1 production by bone marrow-**
124 **derived macrophages.**

125 To investigate how *L. major* impacts innate immune responses elicited by
126 macrophages, we stimulated bone marrow-derived macrophages (BMDM) with
127 lipopolysaccharide (LPS) in the presence or absence of *L. major* (WHOM/IR/-173)
128 infection following established protocol [32]. As detailed in the experimental outline (**Fig.**
129 **1A**), BMDM were stimulated with 20 ng/ml LPS in the presence or absence of 20 MOI *L.*
130 *major* promastigotes for 48 hours. LPS stimulation of BMDM induced robust production
131 of IL-6, TNF and CXCL1. Simultaneous LPS stimulation and *L. major* infection did not
132 impact the production of IL-6 and TNF by BMDM whereas CXCL1 levels were
133 significantly blunted (**Fig. 1A**). These data suggest that *L. major* specifically targets
134 LPS-induced CXCL1 production by BMDM.

135

136 Previous studies have shown that *L. major* targets signaling pathways to evade immune
137 responses and establish infection [[29]]. To examine whether *L. major* specifically
138 targeted CXCL1 expression and production, we designed an experiment whereby
139 BMDM were infected with 20 MOI *L. major* for 6 hours, extracellular *L. major* were
140 washed, then stimulated with 20 ng/ml LPS for the next 42 hours (**Fig. 1B**).
141 Interestingly, *L. major*-infected BMDM produced equal levels of CXCL1 when compared
142 to controls (**Fig. 1B**). These results show that inhibition of CXCL1 by *L. major* may not
143 occur through modulation of intracellular signaling pathway that promotes CXCL1
144 expression and/or production by BMDM.

145

146 **CXCL1 detection is significantly reduced by *L. major* in a cell free system**

147 Given that *L. major* pre-infection of BMDM prior to LPS stimulation did not affect CXCL1
148 production, we posited that *L. major* regulates secreted CXCL1 in the extracellular
149 milieu. To this end, we used supernatants derived from LPS-stimulated BMDM as a
150 source of CXCL1 and cultured 500 μl of these cell-free supernatants with 20×10^6 *L.*
151 *major* promastigotes for 24 hours (**Fig. 2A**). While levels of IL-6 and TNF detected in the
152 supernatants remained unchanged, levels of CXCL1 were significantly reduced after
153 addition of *L. major* to the supernatants. The reduced levels of CXCL1 were not due to
154 its short half-life in the culture, as the levels of CXCL1 in the cell free supernatants were
155 stable up to 48 hours (**Supplemental Fig. 1**). Thus, *L. major* directly dampens CXCL1
156 detection.

157

158 We next examined whether the observed effect of *L. major* on CXCL1 detection was
159 dependent on live parasites. To this end, we cultured supernatants from LPS-stimulated
160 BMDM with *L. major* lysates (*Lm* lysate: generated by 3× freeze-thaw cycles of *L. major*)
161 or supernatants from *L. major* culture (*Lm* sup: supernatant collected from stationary
162 phase of *L. major* growth; **Fig. 2B**). Similar to the addition of live *L. major*, addition of
163 *Lm* lysate or *Lm* sup also reduced CXCL1 in the supernatants while IL-6 and TNF
164 remained unaffected (**Fig. 2B**). These results demonstrate that: first, *L. major* need not
165 be alive to dampen CXCL1 detection; second, *L. major* lysate can dampen CXCL1
166 detection; and finally, *L. major* secreted factors dampen CXCL1 detection. Boiling *Lm*
167 lysate or *Lm* sup for 20 minutes at 100ºC rescued CXCL1 detected in the supernatants,

168 suggesting that the responsible *L. major* components are susceptible to heat treatment
169 (**Supplemental Fig. 2**). Given the sensitivity to heat treatment, we propose that the
170 CXCL1 regulating *L. major* components are proteinaceous.
171

172 ***L. major* reduces recombinant murine CXCL1 (rm-CXCL1) levels in a cell free**
173 **system**

174 Macrophages secrete several hundreds of different proteins that may indirectly alter our
175 observed effect of *L. major* components on CXCL1 [46]. To this end, we obtained
176 recombinant murine CXCL1 (rm-CXCL1, Tonbo Biosciences, San Diego, CA) which
177 was stable in culture up to 48 hours (**Supplemental Fig. 3**). Importantly, *Lm* sup
178 addition to rm-CXCL1 dampened its detection by ELISA in a time-dependent manner,
179 and boiling *Lm* sup rescued rm-CXCL1 detection (**Supplemental Fig. 3**).
180

181 To further investigate the specificity of *L. major* in reducing rm-CXCL1 levels, we
182 examined rm-CXCL2, rh-CXCL1, rh-CXCL2 and rh-CXCL8 sequence homology by
183 CLUSTAL-W alignment and found significant homology between these recombinant
184 proteins. Despite the significant homology, *L. major* failed to reduce levels of rm-
185 CXCL2, rh-CXCL1, rh-CXCL2 or rh-CXCL8, demonstrating specific regulation of rm-
186 CXCL1 (**Fig. 3, B-F**). As expected, *L. major* did not inhibit rm-TNF levels (**Fig. 3G**).
187 Given the specific nature of *L. major* (WHOM/IR/-170) in dampening rm-CXCL1 levels,
188 we next determined whether this activity was specific to the WHOM/IR/-170 isolate.
189 However, supernatant from *L. major* (IA0, isolated from a patient in Iowa who acquired
190 *L. major* in Iraq [47]) was also able to inhibit rm-CXCL1 detection when compared to the

191 WHOM/IR/-170 strain (**Fig. 3H**). Furthermore, exosomes from the *L. major* supernatants
192 from both isolates were able to reduce rm-CXCL1 levels, suggesting that the active
193 components are also present in the *L. major*-derived vesicles (**Fig. 3H**).
194

195 ***L. major* inactivates biological activity of CXCL1**

196 Our data show that *L. major* reduced CXCL1 levels as demonstrated by ELISA (**Figs. 1-**
197 **3**). Possible reasons why CXCL1 levels were reduced when incubated with *L. major*
198 include: 1) *L. major* proteins bind to CXCL1, limiting the ability of anti-CXCL1 antibody in
199 ELISA to interact with CXCL1 or 2) *L. major* proteases cleaves and degrades CXCL1.
200 Considering both outcomes, it is possible that CXCL1, either masked or cleaved by *L.*
201 *major* components, could still be biologically active. To this end, we performed a
202 functional assay where rm-CXCL1 or rm-CXCL1+*Lm* lysate was used to stimulate
203 BMDM (**Fig. 4A**). As demonstrated previously, when rm-CXCL1 is incubated with *L.*
204 *major*, rm-CXCL1 levels are significantly reduced (**Fig. 4B**). *Lm* lysate alone has very
205 little stimulatory activity as demonstrated by mRNA induction of *Cxcl1*, *Tnf* and *Il6* (**Fig.**
206 **4, C-E**). As expected, rm-CXCL1 induced modest increase of *Cxcl1*, *Tnf* and *Il6* but rm-
207 CXCL1+*Lm* lysate failed to induce *Cxcl1*, *Tnf* and *Il6* mRNA (**Fig. 4, C-E**). These results
208 altogether demonstrate that *L. major* inactivates biological activity of rm-CXCL1.
209

210 ***L. major* cleaves CXCL1 at the C-terminal end to promote its degradation**

211 To determine whether CXCL1 is degraded by *L. major*, we incubated rm-CXCL1 with
212 *Lm* lysate for various time periods and examined rm-CXCL1 by silver staining (**Fig. 5A**).
213 Rm-CXCL1 was detected at approximately 10KDa by silver stain. Interestingly, when

214 incubated with *Lm* lysate rm-CXCL1 showed two bands as early as 30 minutes after
215 incubation, suggesting *Lm* lysate-mediated cleavage of rm-CXCL1 (**Fig. 5A and**
216 **Supplemental Fig. 4**). By 2 hours, only the cleaved rm-CXCL1 was observed and this
217 cleaved band intensity decreased over time, suggesting further degradation (**Fig. 5A**).
218 *L. major*-mediated cleavage of rm-CXCL1 was specific because similar experiments
219 done with rm-CXCL2, rh-CXCL1 and rh-CXCL2 did not result in cleavage or
220 degradation of these recombinant proteins (**Fig. 5B**).
221
222 Based on the cleavage pattern of rm-CXCL1 (less than 1KDa shift), cleavage either at
223 the N-terminal or C-terminal end would result in a large fragment (detected by silver
224 stain as the lower band, **Fig. 5A**) and a smaller fragment (which could not be detected
225 by silver stain; **Fig. 5C**). To identify the cleavage product and site, we processed the
226 full-length rm-CXCL1 and *Lm* lysate-cleaved rm-CXCL1 bands by trypsin digestion and
227 performed mass spectrometry to determine the sequence of the bands (**Supplemental**
228 **Fig. 5**). The tryptic peptide sequence readouts of full-length rm-CXCL1 covered the
229 whole rm-CXCL1 peptide sequence (**Supplemental Fig. 5B**), while the peptide
230 coverage of cleaved rm-CXCL1 covered all of the rm-CXCL1 peptide sequence except
231 the last 7 amino acids (MLKGVPK) at the C-terminal end (**Supplemental Fig. 5C**).
232 Thus, *L. major* cleaves rm-CXCL1 after lysine 65 (K65) residue that results in a large N-
233 terminal rm-CXCL1 fragment lacking 7 amino acids at the C-terminal end (**Fig. 5D**).
234
235 ***L. major* metalloprotease cleaves CXCL1**

236 *L. major* has several proteases that enable it to survive within a cell and establish
237 infection [48]. Metalloproteases and cysteine, serine and aspartic proteases are the
238 major proteases described in *L. major* [48]. To examine whether cleavage activity was
239 dependent on proteases, we first treated our rm-CXCL1 + *Lm* sup culture with pan
240 protease inhibitor (Roche and Sigma) (**Fig.6, A-C**). Roche cOmplete protease inhibitor
241 is a broad inhibitor of proteases including serine, cysteine and metalloproteases, and
242 Sigma P8340 inhibitor is reported to inhibit serine, cysteine, acid proteases and
243 aminopeptidases. However, the presence of protease inhibitors from Roche (cOmplete)
244 or Sigma (P8340) did not inhibit *Lm* sup-mediated degradation of rm-CXCL1 as
245 demonstrated by ELISA (**Fig. 6, B and C, and Supplemental Fig. 6**). Marimastat, a
246 broad inhibitor of matrix metalloproteases [49], did not rescue the degradation of rm-
247 CXCL1 by *Lm* sup (**Supplemental Fig. 6B**). EDTA treatment, which chelates metal ions
248 such as Ca^{2+} and Fe^{3+} (and thus can inhibit certain metalloprotease), did not rescue rm-
249 CXCL1 cleavage by *Lm* sup (**Fig. 6, D and E**). Interestingly, 1,10-Phenanthroline, a
250 Zn^{2+} metalloprotease inhibitor [50], rescued rm-CXCL1 degradation by *Lm* sup (**Fig. 6, F**
251 **and G**). While the addition of 1,10-Phenanthroline resulted in the upward shift of rm-
252 CXCL1 bands in SDS-PAGE gels; importantly, no cleavage or degradation of rm-
253 CXCL1 was observed (**Fig. 6G**).
254
255 Several studies have shown that 1,10-Phenanthroline inhibits GP63, a Zn^{2+}
256 metalloprotease present on all *Leishmania spp* and is often used in biochemical assays
257 to inhibit non-specific proteolytic activity of GP63 [51]. To determine whether GP63 was
258 involved in specific cleavage of rm-CXCL1, we immunoprecipitated (IP) GP63 from *Lm*

259 lysate using anti-GP63 antibody (**Fig. 6H**). Immunoblotting the GP63+ve and GP63-ve
260 IP fractions for GP63 showed that GP63 was exclusively present in the IP+ve fraction
261 and not present in the IP-ve fraction demonstrating successful immunoprecipitation of
262 GP63 (**Fig. 6H**). More importantly, when these fractions were cultured with rm-CXCL1,
263 the IP-ve (*Lm* lysate lacking GP63) but not the IP+ve (i.e. GP63) fraction degraded rm-
264 CXCL1 suggesting a role for GP63-independent metalloprotease in the specific
265 degradation of rm-CXCL1 (**Fig. 6I**).
266

267 **Synthetic peptide spanning the CXCL1 cleavage site inhibits *L. major* proteolytic**
268 **activity against rm-CXCL1**

269 Our data suggest that *L. major* Zn^{2+} metalloprotease specifically cleaves rm-CXCL1
270 after the K65 residue leaving a 7-mer amino acid sequence (MLKGVPK). To further
271 examine the specificity of this *L. major* metalloprotease, we designed a blocking peptide
272 that covered this cleavage site (i.e. the last 15 amino acid sequences of rm-CXCL1; **Fig.**
273 **7A**). The addition of blocking peptide was able to rescue *Lm* lysate-mediated
274 degradation of rm-CXCL1 in a dose-dependent manner (**Fig. 7B**). The peptide
275 sequence from the signal peptide region of rm-CXCL1 (peptide #1 and peptide #2, Fig.
276 7A) did not inhibit *Lm* lysate-mediated degradation of rm-CXCL1, demonstrating the
277 specificity of the blocking peptide (**Fig. 7B**). These data demonstrate that a synthetic
278 peptide spanning the murine CXCL1 cleavage site can competitively inhibit *L. major*-
279 mediated rm-CXCL1 degradation.
280

281 **Discussion**

282 CXCL1 is a potent neutrophil chemoattractant and is rapidly upregulated following
283 *Leishmania spp.* infection in the skin [36]; however, the role of CXCL1 during
284 *Leishmania spp.* infection of mice in vivo has been understudied. Charmoy et al showed
285 that mice deficient in CXCL1 have a slight increase in lesion size and reduced numbers
286 of neutrophil infiltrates in chronic lesions, but the overall pathology remained similar
287 between WT and *Cxcl1*$^{-/-}$ mice [33]. However, it should be noted that the study used the
288 *L. major* Seidman strain (*Lm*Sd) that causes a non-healing infection in C57BL/6 mice
289 [33]. Thus, more thorough analyses are needed to determine the precise role of CXCL1
290 during *L. major* infection in mice and humans.
291
292 Importantly, even depletion of neutrophils using anti-Gr1 neutralizing antibody does not
293 always lead to increased parasitic burden, lesion or pathology [21]. While some studies
294 with acute depletion of neutrophils reported worsened pathology during *L. major*
295 infections, other studies have shown no role or even amelioration of disease pathology
296 [5, 52-60]. Thus, mouse strain, *L. major* strain, route of infection and timing of CXCL1
297 release may all contribute to the fate of the infection and overall pathology. In line with
298 this thought, two independent *L. major* strains were tested in our study, and both strains
299 degraded CXCL1 in our experimental systems. Whether this degradation of murine
300 CXCL1 is a specific feature of *L. major* or a more general feature of all *Leishmania spp.*
301 will need further investigation.
302

303 Our initial observation demonstrated that *L. major* in culture with macrophages
304 effectively inhibited LPS-induced CXCL1 production. Further examination showed that
305 intracellular *L. major* within the macrophages did not inhibit LPS-induced CXCL1
306 production. These experiments suggest that *L. major* does not interfere with signaling
307 pathways that promote CXCL1 production but directly regulates secreted CXCL1 in the
308 extracellular milieu. *L. major* are present as metacyclic promastigotes in sandflies [61].
309 When infected into the mammalian host, *L. major* infect macrophages and resides
310 within the vacuole where they transform into amastigotes, multiply and establish
311 infection [62]. Because *L. major*-infected macrophages which contain amastigotes did
312 not inhibit CXCL1 production, it could be posited that only the promastigote form of *L.*
313 *major* degrades CXCL1. However, genome microarray analysis shows that the majority
314 of genes are constitutively expressed in both *L. major* promastigotes and amastigotes
315 (>90%) and therefore the major genes and virulent factors expressed by these different
316 stages of *L. major* may not be different [63]. Thus, both *L. major* promastigotes and
317 amastigotes may similarly cleave and degrade murine CXCL1 in an in vitro assay. In
318 addition, infected macrophages can secrete exosomes containing *L. major* proteins [64,
319 65], which could degrade murine CXCL1. We have consistently shown that *L. major*
320 secreted microvesicles (i.e. exosomes) contain these metalloproteases that can
321 degrade murine CXCL1. Physiologically, *L. major* promastigotes released during a
322 sandfly bite may act locally to limit acute CXCL1 produced in response to the infection.
323 Once *L. major* are phagocytosed and transformed into amastigotes, they are physically
324 separated from the CXCL1 due to their location (amastigotes are in the vacuole while

325 CXCL1 are secreted by the macrophages and are extracellular) and may only impact
326 CXCL1 production through the *L. major* component laden exosomes.
327
328 Our studies suggest that a yet-unknown metalloprotease from *L. major* cleaves murine
329 CXCL1. Given that 1,10-Phenanthroline (Zn^{2+} chelator) but not EDTA (Ca^{2+} and Fe^{3+}
330 metal ion chelator) or Marimastat (Matrix metalloprotease inhibitor) rescued *L. major*-
331 mediated CXCL1 degradation, it is possible that the unknown metalloprotease is a Zn^{2+}
332 metalloprotease. Our studies also demonstrate that the *L. major* metalloprotease is
333 highly specific for murine CXCL1 in that its closest murine homolog, CXCL2, or human
334 homologs, CXCL1, CXCL2 or CXCL8, were not degraded. We hypothesize that this
335 particular *L. major* metalloprotease may have evolved to specifically evade host immune
336 response in rodents. Given that human CXCL1 homologs are not susceptible to this
337 metalloprotease, one can argue that our results may not have any importance from a
338 public health standpoint, but we reason otherwise. Our results are highly relevant to
339 public health because rodents are ubiquitous, serve as a reservoir for *Leishmania spp*.
340 and we highlight a rodent-specific *L. major* evolution in targeting murine CXCL1 [66].
341
342 Our studies demonstrate that the murine CXCL1 is first cleaved at the C-terminal end
343 after K65 releasing a 7aa residue. CXCL1 cleavage occurs as early as 30 minutes of
344 incubation with *L. major* and by 4 hours the cleavage is complete in that only the
345 cleaved bands are observed. Interestingly, we did not observe any accumulation of the
346 cleaved CXCL1 band, suggesting continuous degradation of the cleaved form. While
347 our data clearly demonstrate that the unknown *L. major* metalloprotease mediates

348 cleavage of murine CXCL1, how the cleaved CXCL1 is further degraded will be the
349 subject of future investigation. The cleaved murine CXCL1 (lacking the C-terminal 7 aa)
350 may be highly unstable and undergo spontaneous degradation overtime. Alternatively,
351 the cleaved murine CXCL1 may be susceptible to additional *L. major* proteases which
352 promote its subsequent degradation.
353
354 In conclusion, we have identified an immune evasion strategy utilized by *L. major* that is
355 highly specific to murine CXCL1 (**Fig. 7C**). Specifically, *L. major*-associated
356 metalloprotease cleaved murine CXCL1 at K65 residue and released a C-terminal 7
357 amino acid fragment to promote its degradation. Finally, we have designed a peptide
358 spanning the cleavage site of CXCL1 that inhibited murine CXCL1 cleavage by *L.*
359 *major*. Our study altogether uncovered an immune evasion strategy employed by *L.*
360 *major* that may have evolved in rodents and highlights how parasites may utilize diverse
361 immune evasion strategy to establish infection within its diverse mammalian hosts.
362

363 **Methods**

364 **Ethics statement**

365 Experimental procedures that utilized mice were all approved by the University of Iowa
366 Animal Care and Use Committee (Approved Animal Protocol # 7042004 – PI Dr.
367 Prajwal Gurung) and performed in accordance to the Office of Laboratory Animal
368 Welfare guidelines and the PHS Policy on Humane Care and Use of Laboratory
369 Animals.

370

371 **BMDM culture**

372 BMDMs were prepared as described previously (32). Briefly, bone marrow cells were
373 harvested from the hind limbs of BALB/c mice (Jackson Laboratory, Stock No. 000651)
374 and cultured in L cell-conditioned IMDM medium supplemented with 10% FBS, 1%
375 nonessential amino acid, and 1% penicillin-streptomycin for 5-7 d to differentiate into
376 macrophages. BMDMs were counted and seeded at 1×10^6 cells in 12-well cell culture
377 plates in IMDM media containing 10% FBS, 1% nonessential amino acids, and 1%
378 penicillin-streptomycin. BMDMs were primed with LPS (20 ng/ml) and infected with 20
379 MOI *L. major* promastigotes for 24 and 48 hours (Supplemental Figure 1). For some
380 experiments, BMDMs were LPS primed to generate supernatant containing cytokines
381 for in vitro biochemical analysis with *L. major* supernatant (*Lm* sup) and *L. major* lysate
382 (*Lm* lysate). BMDMs were also treated with rm-CXCL1 (20 ng/ml) or rm-CXCL1+*Lm* sup
383 preparations in some experiments.

384

385 **L. major culture**

386 *L. major* strains WHOM/IR/-173 [67] and IA0 [47] were grown in T-25 flasks with M199
387 media supplemented with 10% FBS, 5% HEPES and 1% penicillin-streptomycin at room
388 temperature. BMDMs were infected with 20 MOI of *L. major* promastigotes for 48 hours.
389 Conditioned *L. major* supernatant (*Lm* sup) was prepared after *L. major* reached the
390 stable growth phase at approximately 20 × 10^6 / ml. Following centrifugation (3000×g) to
391 pellet *L. major*, supernatants were collected and filtered using a 0.2μm vacuum filter to
392 harvest *Lm* sup. *Lm* lysate was prepared by collecting the *L. major* pellet, washing 3
393 times with PBS followed by 3 freeze-thaw cycles of 7 × 10^9 *L. major* /ml in PBS. For the
394 preparation of *L. major* exosomes, promastigotes were grown to stable phase and
395 changed to serum-free media and incubated at room temperature overnight.
396 Supernatant was obtained as above and then separated using a 100kDa molecular
397 weight Amicon ultra-15 centrifugal filter (MilliporeSigma, Burlington, MA). The
398 concentrated vesicles were washed twice with PBS by ultracentrifugation at 110,000xg
399 at 4°C for 1 hour (Beckman Optma MAX-XP Ultracentrifuge, rotor TLA 120.2; Beckman
400 Coulter Inc., USA). The final pellet (exosomes) was resuspended in PBS and used in in
401 vitro biochemistry assays.
402

403 **Electrophoresis and in vitro biochemistry**

404 For in vitro reactions, 125ng of total recombinant protein was separated on 4-20% or
405 10-20% Novex WedgeWell Tris-Glycine precast gels (Thermofisher, Waltham, MA).
406 For silver stain, the Pierce Mass Spec compatible silver stain kit was used per
407 manufacturer's instructions (Thermofisher). Synthetic peptides were generated and
408 purchased from Pierce Biotechnology (Thermofisher) and are composed of the

409 following sequences: peptide#1: CAALLLLATSRLA; peptide#2: RLATGAPIAN;
410 blocking peptide: LVQKIVQKMLKGVPK. For Western blot analysis a semi-dry transfer
411 was completed using trans-blot turbo system (Bio-Rad, Hercules, CA) with Immobilon
412 PVDF membrane. The membranes were blocked in 5% non-fat milk for 1 hour at room
413 temperature. Membranes were probed with sheep polyclonal antibody Sp180 raised
414 against *L. chagasi* promastigote GP63 at a concentration 1:1500 incubated overnight at
415 4°C. The membranes were then probed with HRP-tagged secondary antibodies at room
416 temperature for 1 hour and developed using Immobilon Forte Western HRP Substrate
417 (MilliporeSigma) and imaged with an Odyssey Fc Infrared Imaging System (LI-COR
418 Bioscience, Lincoln, NE). Immunoprecipitation was performed using Protein G
419 Dynabeads and Leishmania GP63 monoclonal antibody clone 96-126 (Thermofisher).
420 As instructed by the manufacturer, 50μL beads were washed in PBS with 0.02% Tween
421 20 and bound to 5μg antibody for at least 10 minutes. Following a wash, the antibody
422 bound beads were incubated with *Lm* lysate for another 10 minutes and finally either
423 antigen-antibody binding was negated by acidic (pH 2.8) 50mM Glycine treatment or
424 bead bound antibody-antigen complexes were used directly for biochemistry.
425

426 **Mass spectrometry**

427 *In-gel trypsin digestion:* The gel was stained using a Pierce mass spec compatible silver
428 stain kit (Thermofisher) per manufacturer directions. A procedure slightly modified than
429 that described by Yu et al [68] was used for in-gel digestion. Briefly, the targeted protein
430 bands from SDS-PAGE gel were manually excised, cut into 1mm^3 pieces, and washed
431 in 100mM ammonium bicarbonate:acetonitrile (1:1, v/v) and 25mM ammonium

432 bicarbonate /acetonitrile (1:1, v/v), respectively, to achieve complete de-staining. The
433 gel pieces were further treated with acetonitrile (ACN), to effectively “dry” the gel
434 segments and then reduced in 50μl of 10mM DTT at 56 °C for 60 min. Gel-trapped
435 proteins were alkylated with 55mM chloroacetamide (CAM) for 30 min at room
436 temperature. The gel pieces were washed with 25mM ammonium bicarbonate:
437 acetonitrile (1:1, v/v) twice to remove excess DTT and CAM. 50μl of cold trypsin solution
438 at 10ng/μl in 25mM ammonium bicarbonate was then added to the gel pieces and they
439 were allowed to swell on ice for 60 min. Digestion was conducted at 37°C for 16 h.
440 Peptide extraction was performed three times, adding 100μL of 50% acetonitrile/0.1%
441 formic acid for 0.5 h, combining the supernatants. The combined extracts were
442 concentrated in a lyophilizer and rehydrated with 15 μl of mobile phase A.
443
444 *LC-MS/MS*: Mass spectrometry data were collected using an Orbitrap Fusion Lumos
445 mass spectrometer (Thermofisher) coupled to an Easy-nLC-1200™ System (Proxeon
446 P/N LC1400). The autosampler is set to aspirate 3μl (estimated 0.3ug) of reconstituted
447 digest and load the solution on a 2.5cm C18 trap (New Objective, P/N IT100-25H002)
448 coupled to waste, HV or analytical column through a microcross assembly (IDEX, P/N
449 UH-752). Peptides are desalted on the trap using 16μl mobile phase A for 4 min. The
450 waste valve is then blocked and a gradient begins flowing at 0.4μl/min through a self-
451 packed analytical column, 10cm in length × 75μm id. The fused silica column was
452 tapered from 100μm ID (Polymicro) to ~8μm at the tip using a Sutter P-2000 laser puller
453 then packed with 2.7micron Halo C18 particles using a He-pressurized SS cylinder.
454 Peptides were separated in-line with the mass spectrometer using a 70 min gradient

455 composed of linear and static segments wherein buffer A is 0.1% formic acid and B is
456 95%ACN, 0.1% formic acid. The gradient begins first hold at 4% for 3 min then makes
457 the following transitions (%B, min): (2, 0), (35, 46), (60, 56), (98, 62), (98, 70).
458
459 *Tandem mass spectrometry on the Thermo Q-Exactive hf*: Data acquisitions begin with
460 a survey scan (m/z 380 -1800) acquired on a Q-Exactive Orbitrap mass spectrometer
461 (Thermofisher) at a resolution of 120,000 in the off-axis Orbitrap segment (MS1) with
462 automatic gain control (AGC) set to 3E06 and a maximum injection time of 50 ms. MS1
463 scans were acquired every 3 sec during the 70-min gradient described above. The most
464 abundant precursors were selected among 2-6 charge state ions at a 1E05 AGC and 70
465 ms maximum injection time. Ions were isolated with a 1.6 Th window using the multi-
466 segment quadrupole and subjected to dynamic exclusion for 30 sec if they were
467 targeted twice in the prior 30 sec. Selected ions were then subjected to high energy
468 collision-induced dissociation (HCD) in the ion routing multipole (IRM). Targeted
469 precursors were fragmented by (HCD) at 30% collision energy in the IRM. HCD
470 fragment ions were analyzed using the Orbitrap (AGC 1.2E05, maximum injection time
471 110 ms, and resolution set to 30,000 at 400 Th). Both MS2 data were recorded as
472 centroid and the MS1 survey scans were recorded in profile mode.
473
474 *Proteomic searches*: Initial spectral searches were performed with both Mascot version
475 2.6.2 (MatrixScience) and Byonic search engines (Protein Metrics ver. 2.8.2). Search
476 databases were composed of the Uniprot KB for species 10090 (mouse) downloaded
477 February 6, 2016 containing 58436 sequences. In either search, an equal number of

478 decoy entries were created and searched simultaneously by reversing the original
479 entries in the target database. Precursor mass tolerance was set to 5 ppm and
480 fragments were searched at 10 ppm. A fixed 57 Da modification was assumed for
481 cysteine residues while variable oxidation was allowed at methionine. A variable GG
482 modification at lysine was set to monitor ubiquitylation and potential phosphorylation
483 was accessed at Ser and Thr residues. The false discovery rate was maintained at 1%
484 by tracking matches to the decoy database. Both Mascot and Byonic search results
485 were combined and validated using Scaffold ver. 4.8.5 (Proteome Software). Protein
486 assignments required a minimum of two peptides established at 70% probability (local
487 FDR algorithm) and an overall 95% protein probability (assigned by Protein Prophet).
488 Approximately 300 protein families (including common contaminants) were assigned at
489 a total FDR to 1.2%. Proteins were annotated with GO terms from goa_uniprot_all.gaf
490 downloaded on May 3, 2017.
491

492 **Immunoassays and recombinant proteins**

493 Cytokine ELISAs and multiplex immunoassays were performed according to
494 manufacturer instructions. Mouse and human CXCL1 and CXCL2 as well as human IL-
495 8 (CXCL8) were obtained from R&D Systems (Minneapolis, MN) and multiplex CXCL1,
496 IL-6, and TNF were completed using ProcartaPlex assays (Thermofisher) which were
497 run on the BioRad Bio-Plex (Luminex, Austin, TX). We obtained our recombinant
498 proteins from Tonbo biosciences which included mouse CXCL1, CXCL2, and TNF as
499 well as human CXCL1, CXCL2, and CXCL8.
500

501 **PCR methods**

502 RNA was extracted from BMDM cultures in TRIzol reagent (Thermofisher) followed by
503 chloroform extraction and isopropanol precipitation. The extracted RNA was reverse-
504 transcribed into cDNA by using qScript Supermix (Quanta Biosciences, Beverly, MA).
505 Real-time quantitative PCR was performed on Eppendorf realplex EPgradient S
506 Mastercycler (Eppendorf, Germany) using PerfeCTa SYBR Green SuperMix ROX
507 (Quanta Biosciences) and the appropriate primers. The sequences of the quantitative
508 RT-PCR primers are as follows: *mCXCL1:* 5'-CAATGAGCTGCGCTGTCAGTG-3', 5'-
509 CTTGGGGACACCTTTTAGCATC-3'; *mTnf*: 5′-CATCTTCTCAAAATTCGAGTGACAA-
510 3′, 5′-TGGGAGTAGACAAGGTACAACCC-3′; *mIL-6:* 5'-
511 CAAGAAAGACAAAGCCAGAGTC-3', 5'-GAAATTGGGGTAGGAAGGAC-3'.
512 Threshold cycle Ct values were normalized to GAPDH, and gene fold change was
513 determined by the relative comparison method, relative to the 0 h time point.
514

515 **Statistical analysis and alignment**

516 GraphPad Prism 8.0 software was used for data analysis and figure presentation. Data
517 are shown as mean ± SEM. Statistical significance was determined by *t* tests (two-tailed
518 and Mann-Whitney) for two groups, and one-way ANOVA (with Dunnett's or Tukey's
519 multiple comparisons tests) for three or more groups. For the purpose of alignment
520 presentation, sequences were obtained from the protein manufacturer or the NCBI
521 protein database and figures were prepared using Jalview 2 [69].
522

523 **Authorships**

524 M.S.Y, B.P., L.M. performed the experiments. M.S.Y, M.E.W., and P.G. analyzed the
525 data. R.M.P. performed the mass spectrometry and analysis of CXCL1 cleavage bands.
526 M.S.Y. and P.G. wrote the manuscript with input from all authors. P.G. designed and
527 conceptualized the study.

528

529 **Acknowledgements**

530 We thank the University of Iowa Proteomics Core for the comparative analysis
531 performed in the University of Iowa Proteomic facility, Directed by RMP and supported
532 by an endowment from the Carver Foundation and by Thermo Lumos provided through
533 an HHMI grant to Dr. Kevin Campbell. We thank Kristina Greiner for her help with
534 scientific editing of the manuscript. We are also thankful to the members of the
535 Inflammation Program for critical insights provided during the development of the
536 project. This work was supported by NIAID K22AI127836 Grant, NIEHS P30ES005605
537 Pilot Grant, and the University of Iowa Startup funds to Dr. Prajwal Gurung.

538

539 **Conflict of Interest**

540 The authors have no conflict of interest to declare.

541

542

543 **References**
544
545 1. Elnaiem DE. Ecology and control of the sand fly vectors of Leishmania donovani
546 in East Africa, with special emphasis on Phlebotomus orientalis. J Vector Ecol. 2011;36
547 Suppl 1:S23-31. Epub 2011/03/05. doi: 10.1111/j.1948-7134.2011.00109.x. PubMed
548 PMID: 21366778.
549 2. Ehrchen JM, Roebrock K, Foell D, Nippe N, von Stebut E, Weiss JM, et al.
550 Keratinocytes determine Th1 immunity during early experimental leishmaniasis. PLoS
551 Pathog. 2010;6(4):e1000871. Epub 2010/05/06. doi: 10.1371/journal.ppat.1000871.
552 PubMed PMID: 20442861; PubMed Central PMCID: PMCPMC2861693.
553 3. Scorza BM, Wacker MA, Messingham K, Kim P, Klingelhutz A, Fairley J, et al.
554 Differential Activation of Human Keratinocytes by Leishmania Species Causing
555 Localized or Disseminated Disease. J Invest Dermatol. 2017;137(10):2149-56. Epub
556 2017/06/26. doi: 10.1016/j.jid.2017.05.028. PubMed PMID: 28647347; PubMed Central
557 PMCID: PMCPMC5786447.
558 4. Ribeiro-Gomes FL, Moniz-de-Souza MC, Alexandre-Moreira MS, Dias WB,
559 Lopes MF, Nunes MP, et al. Neutrophils activate macrophages for intracellular killing of
560 Leishmania major through recruitment of TLR4 by neutrophil elastase. J Immunol.
561 2007;179(6):3988-94. Epub 2007/09/06. PubMed PMID: 17785837.
562 5. Ribeiro-Gomes FL, Otero AC, Gomes NA, Moniz-De-Souza MC, Cysne-
563 Finkelstein L, Arnholdt AC, et al. Macrophage interactions with neutrophils regulate
564 Leishmania major infection. J Immunol. 2004;172(7):4454-62. Epub 2004/03/23.
565 PubMed PMID: 15034061.

566 6. Liu D, Uzonna JE. The early interaction of Leishmania with macrophages and
567 dendritic cells and its influence on the host immune response. Front Cell Infect
568 Microbiol. 2012;2:83. Epub 2012/08/25. doi: 10.3389/fcimb.2012.00083. PubMed PMID:
569 22919674; PubMed Central PMCID: PMCPMC3417671.
570 7. Gurung P, Kanneganti TD. Innate immunity against Leishmania infections. Cell
571 Microbiol. 2015;17(9):1286-94. Epub 2015/08/08. doi: 10.1111/cmi.12484. PubMed
572 PMID: 26249747; PubMed Central PMCID: PMCPMC4698274.
573 8. Kaye P, Scott P. Leishmaniasis: complexity at the host-pathogen interface. Nat
574 Rev Microbiol. 2011;9(8):604-15. Epub 2011/07/13. doi: 10.1038/nrmicro2608. PubMed
575 PMID: 21747391.
576 9. Naderer T, Heng J, Saunders EC, Kloehn J, Rupasinghe TW, Brown TJ, et al.
577 Intracellular Survival of Leishmania major Depends on Uptake and Degradation of
578 Extracellular Matrix Glycosaminoglycans by Macrophages. PLoS Pathog.
579 2015;11(9):e1005136. Epub 2015/09/04. doi: 10.1371/journal.ppat.1005136. PubMed
580 PMID: 26334531; PubMed Central PMCID: PMCPMC4559419.
581 10. Avila-Garcia M, Mancilla-Ramirez J, Segura-Cervantes E, Farfan-Labonne B,
582 Ramirez-Ramirez A, Galindo-Sevilla N. Transplacental transmission of cutaneous
583 Leishmania mexicana strain in BALB/c mice. Am J Trop Med Hyg. 2013;89(2):354-8.
584 Epub 2013/06/27. doi: 10.4269/ajtmh.12-0716. PubMed PMID: 23798582; PubMed
585 Central PMCID: PMCPMC3741259.
586 11. Ben Slimane T, Chouihi E, Ben Hadj Ahmed S, Chelbi I, Barhoumi W, Cherni S,
587 et al. An investigation on vertical transmission of Leishmania infantum in experimentally
588 infected dogs and assessment of offspring's infectiousness potential by xenodiagnosis.

589 Vet Parasitol. 2014;206(3-4):282-6. Epub 2014/12/04. doi:
590 10.1016/j.vetpar.2014.10.020. PubMed PMID: 25468025.
591 12. da Silva SM, Ribeiro VM, Ribeiro RR, Tafuri WL, Melo MN, Michalick MS. First
592 report of vertical transmission of Leishmania (Leishmania) infantum in a naturally
593 infected bitch from Brazil. Vet Parasitol. 2009;166(1-2):159-62. Epub 2009/09/08. doi:
594 10.1016/j.vetpar.2009.08.011. PubMed PMID: 19733439.
595 13. Naucke TJ, Lorentz S. First report of venereal and vertical transmission of canine
596 leishmaniosis from naturally infected dogs in Germany. Parasit Vectors. 2012;5:67.
597 Epub 2012/04/03. doi: 10.1186/1756-3305-5-67. PubMed PMID: 22463789; PubMed
598 Central PMCID: PMCPMC3350385.
599 14. Gibson-Corley KN, Hostetter JM, Hostetter SJ, Mullin K, Ramer-Tait AE,
600 Boggiatto PM, et al. Disseminated Leishmania infantum infection in two sibling
601 foxhounds due to possible vertical transmission. Can Vet J. 2008;49(10):1005-8. Epub
602 2009/01/03. PubMed PMID: 19119370; PubMed Central PMCID: PMCPMC2553493.
603 15. Rosypal AC, Troy GC, Duncan RB, Zajac AM, Lindsay DS. Utility of diagnostic
604 tests used in diagnosis of infection in dogs experimentally inoculated with a North
605 American isolate of Leishmania infantum infantum. J Vet Intern Med. 2005;19(6):802-9.
606 Epub 2005/12/17. PubMed PMID: 16355672.
607 16. Swenson CL, Silverman J, Stromberg PC, Johnson SE, Wilkie DA, Eaton KA, et
608 al. Visceral leishmaniasis in an English foxhound from an Ohio research colony. J Am
609 Vet Med Assoc. 1988;193(9):1089-92. Epub 1988/11/01. PubMed PMID: 3198462.
610 17. Petersen CA, Barr SC. Canine leishmaniasis in North America: emerging or
611 newly recognized? Vet Clin North Am Small Anim Pract. 2009;39(6):1065-74, vi. Epub

612 2009/11/26. doi: 10.1016/j.cvsm.2009.06.008. PubMed PMID: 19932363; PubMed
613 Central PMCID: PMCPMC2824922.
614 18. Ashford RW. Leishmaniasis reservoirs and their significance in control. Clin
615 Dermatol. 1996;14(5):523-32. Epub 1996/09/01. PubMed PMID: 8889331.
616 19. Oghumu S, Lezama-Davila CM, Isaac-Marquez AP, Satoskar AR. Role of
617 chemokines in regulation of immunity against leishmaniasis. Exp Parasitol.
618 2010;126(3):389-96. Epub 2010/03/09. doi: 10.1016/j.exppara.2010.02.010. PubMed
619 PMID: 20206625; PubMed Central PMCID: PMCPMC3661772.
620 20. Charmoy M, Auderset F, Allenbach C, Tacchini-Cottier F. The prominent role of
621 neutrophils during the initial phase of infection by Leishmania parasites. J Biomed
622 Biotechnol. 2010;2010:719361. Epub 2009/11/04. doi: 10.1155/2010/719361. PubMed
623 PMID: 19884987; PubMed Central PMCID: PMCPMC2768872.
624 21. Ribeiro-Gomes FL, Sacks D. The influence of early neutrophil-Leishmania
625 interactions on the host immune response to infection. Front Cell Infect Microbiol.
626 2012;2:59. Epub 2012/08/25. doi: 10.3389/fcimb.2012.00059. PubMed PMID:
627 22919650; PubMed Central PMCID: PMCPMC3417510.
628 22. Chang KP, McGwire BS. Molecular determinants and regulation of Leishmania
629 virulence. Kinetoplastid Biol Dis. 2002;1(1):1. Epub 2002/09/18. PubMed PMID:
630 12234388; PubMed Central PMCID: PMCPMC119322.
631 23. Joshi PB, Kelly BL, Kamhawi S, Sacks DL, McMaster WR. Targeted gene
632 deletion in Leishmania major identifies leishmanolysin (GP63) as a virulence factor. Mol
633 Biochem Parasitol. 2002;120(1):33-40. Epub 2002/02/19. PubMed PMID: 11849703.

634 24. Spath GF, Lye LF, Segawa H, Sacks DL, Turco SJ, Beverley SM. Persistence
635 without pathology in phosphoglycan-deficient Leishmania major. Science.
636 2003;301(5637):1241-3. Epub 2003/08/30. doi: 10.1126/science.1087499. PubMed
637 PMID: 12947201.
638 25. Brittingham A, Morrison CJ, McMaster WR, McGwire BS, Chang KP, Mosser
639 DM. Role of the Leishmania surface protease gp63 in complement fixation, cell
640 adhesion, and resistance to complement-mediated lysis. J Immunol. 1995;155(6):3102-
641 11. Epub 1995/09/15. PubMed PMID: 7673725.
642 26. Puentes SM, Sacks DL, da Silva RP, Joiner KA. Complement binding by two
643 developmental stages of Leishmania major promastigotes varying in expression of a
644 surface lipophosphoglycan. J Exp Med. 1988;167(3):887-902. Epub 1988/03/01.
645 PubMed PMID: 3280727; PubMed Central PMCID: PMCPMC2188887.
646 27. Desjardins M, Descoteaux A. Inhibition of phagolysosomal biogenesis by the
647 Leishmania lipophosphoglycan. J Exp Med. 1997;185(12):2061-8. Epub 1997/06/16.
648 PubMed PMID: 9182677; PubMed Central PMCID: PMCPMC2196352.
649 28. Vinet AF, Fukuda M, Turco SJ, Descoteaux A. The Leishmania donovani
650 lipophosphoglycan excludes the vesicular proton-ATPase from phagosomes by
651 impairing the recruitment of synaptotagmin V. PLoS Pathog. 2009;5(10):e1000628.
652 Epub 2009/10/17. doi: 10.1371/journal.ppat.1000628. PubMed PMID: 19834555;
653 PubMed Central PMCID: PMCPMC2757729.
654 29. Gupta G, Oghumu S, Satoskar AR. Mechanisms of immune evasion in
655 leishmaniasis. Adv Appl Microbiol. 2013;82:155-84. Epub 2013/02/19. doi:

656 10.1016/B978-0-12-407679-2.00005-3. PubMed PMID: 23415155; PubMed Central
657 PMCID: PMCPMC3697132.
658 30. Isnard A, Shio MT, Olivier M. Impact of Leishmania metalloprotease GP63 on
659 macrophage signaling. Front Cell Infect Microbiol. 2012;2:72. Epub 2012/08/25. doi:
660 10.3389/fcimb.2012.00072. PubMed PMID: 22919663; PubMed Central PMCID:
661 PMCPMC3417651.
662 31. Gantt KR, Schultz-Cherry S, Rodriguez N, Jeronimo SM, Nascimento ET,
663 Goldman TL, et al. Activation of TGF-beta by Leishmania chagasi: importance for
664 parasite survival in macrophages. J Immunol. 2003;170(5):2613-20. Epub 2003/02/21.
665 PubMed PMID: 12594289.
666 32. Gurung P, Karki R, Vogel P, Watanabe M, Bix M, Lamkanfi M, et al. An NLRP3
667 inflammasome-triggered Th2-biased adaptive immune response promotes
668 leishmaniasis. J Clin Invest. 2015;125(3):1329-38. Epub 2015/02/18. doi:
669 10.1172/JCI79526. PubMed PMID: 25689249; PubMed Central PMCID:
670 PMCPMC4362229.
671 33. Charmoy M, Hurrell BP, Romano A, Lee SH, Ribeiro-Gomes F, Riteau N, et al.
672 The Nlrp3 inflammasome, IL-1beta, and neutrophil recruitment are required for
673 susceptibility to a nonhealing strain of Leishmania major in C57BL/6 mice. Eur J
674 Immunol. 2016;46(4):897-911. Epub 2015/12/23. doi: 10.1002/eji.201546015. PubMed
675 PMID: 26689285; PubMed Central PMCID: PMCPMC4828310.
676 34. WHO. Leishmaniasis. https://wwwwhoint/news-room/fact-
677 sheets/detail/leishmaniasis. 2018;World Health Orgnaization.

678 35. Teixeira MJ, Teixeira CR, Andrade BB, Barral-Netto M, Barral A. Chemokines in
679 host-parasite interactions in leishmaniasis. Trends Parasitol. 2006;22(1):32-40. Epub
680 2005/11/29. doi: 10.1016/j.pt.2005.11.010. PubMed PMID: 16310413.
681 36. Muller K, van Zandbergen G, Hansen B, Laufs H, Jahnke N, Solbach W, et al.
682 Chemokines, natural killer cells and granulocytes in the early course of Leishmania
683 major infection in mice. Med Microbiol Immunol. 2001;190(1-2):73-6. Epub 2002/01/05.
684 PubMed PMID: 11770115.
685 37. Modi WS, Yoshimura T. Isolation of novel GRO genes and a phylogenetic
686 analysis of the CXC chemokine subfamily in mammals. Mol Biol Evol. 1999;16(2):180-
687 93. Epub 1999/02/24. doi: 10.1093/oxfordjournals.molbev.a026101. PubMed PMID:
688 10028286.
689 38. Bozic CR, Kolakowski LF, Jr., Gerard NP, Garcia-Rodriguez C, von Uexkull-
690 Guldenband C, Conklyn MJ, et al. Expression and biologic characterization of the
691 murine chemokine KC. J Immunol. 1995;154(11):6048-57. Epub 1995/06/01. PubMed
692 PMID: 7751647.
693 39. Chintakuntlawar AV, Chodosh J. Chemokine CXCL1/KC and its receptor CXCR2
694 are responsible for neutrophil chemotaxis in adenoviral keratitis. J Interferon Cytokine
695 Res. 2009;29(10):657-66. Epub 2009/08/01. doi: 10.1089/jir.2009.0006. PubMed PMID:
696 19642907; PubMed Central PMCID: PMCPMC2956677.
697 40. Frevert CW, Huang S, Danaee H, Paulauskis JD, Kobzik L. Functional
698 characterization of the rat chemokine KC and its importance in neutrophil recruitment in
699 a rat model of pulmonary inflammation. J Immunol. 1995;154(1):335-44. Epub
700 1995/01/01. PubMed PMID: 7995953.

701 41. Girbl T, Lenn T, Perez L, Rolas L, Barkaway A, Thiriot A, et al. Distinct
702 Compartmentalization of the Chemokines CXCL1 and CXCL2 and the Atypical
703 Receptor ACKR1 Determine Discrete Stages of Neutrophil Diapedesis. Immunity.
704 2018;49(6):1062-76 e6. Epub 2018/11/18. doi: 10.1016/j.immuni.2018.09.018. PubMed
705 PMID: 30446388; PubMed Central PMCID: PMCPMC6303217.
706 42. van Zandbergen G, Hermann N, Laufs H, Solbach W, Laskay T. Leishmania
707 promastigotes release a granulocyte chemotactic factor and induce interleukin-8 release
708 but inhibit gamma interferon-inducible protein 10 production by neutrophil granulocytes.
709 Infect Immun. 2002;70(8):4177-84. Epub 2002/07/16. PubMed PMID: 12117926;
710 PubMed Central PMCID: PMCPMC128123.
711 43. Badolato R, Sacks DL, Savoia D, Musso T. Leishmania major: infection of human
712 monocytes induces expression of IL-8 and MCAF. Exp Parasitol. 1996;82(1):21-6. Epub
713 1996/01/01. doi: 10.1006/expr.1996.0003. PubMed PMID: 8617327.
714 44. Racoosin EL, Beverley SM. Leishmania major: promastigotes induce expression
715 of a subset of chemokine genes in murine macrophages. Exp Parasitol. 1997;85(3):283-
716 95. Epub 1997/03/01. doi: 10.1006/expr.1996.4139. PubMed PMID: 9085925.
717 45. Wilson ME, Innes DJ, Sousa AD, Pearson RD. Early histopathology of
718 experimental infection with Leishmania donovani in hamsters. J Parasitol.
719 1987;73(1):55-63. Epub 1987/02/01. PubMed PMID: 3572666.
720 46. Koppenol-Raab M, Sjoelund V, Manes NP, Gottschalk RA, Dutta B, Benet ZL, et
721 al. Proteome and Secretome Analysis Reveals Differential Post-transcriptional
722 Regulation of Toll-like Receptor Responses. Mol Cell Proteomics. 2017;16(4 suppl

723 1):S172-S86. Epub 2017/02/27. doi: 10.1074/mcp.M116.064261. PubMed PMID:
724 28235783; PubMed Central PMCID: PMCPMC5393387.
725 47. Clay GM, Valadares DG, Graff JW, Ulland TK, Davis RE, Scorza BM, et al. An
726 Anti-Inflammatory Role for NLRP10 in Murine Cutaneous Leishmaniasis. J Immunol.
727 2017;199(8):2823-33. Epub 2017/09/22. doi: 10.4049/jimmunol.1500832. PubMed
728 PMID: 28931602; PubMed Central PMCID: PMCPMC5679237.
729 48. Silva-Almeida M, Souza-Silva F, Pereira BA, Ribeiro-Guimaraes ML, Alves CR.
730 Overview of the organization of protease genes in the genome of Leishmania spp.
731 Parasit Vectors. 2014;7:387. Epub 2014/08/22. doi: 10.1186/1756-3305-7-387. PubMed
732 PMID: 25142315; PubMed Central PMCID: PMCPMC4158035.
733 49. Rasmussen HS, McCann PP. Matrix metalloproteinase inhibition as a novel
734 anticancer strategy: a review with special focus on batimastat and marimastat.
735 Pharmacol Ther. 1997;75(1):69-75. Epub 1997/01/01. PubMed PMID: 9364582.
736 50. Day TA, Chen GZ. The metalloprotease inhibitor 1,10-phenanthroline affects
737 Schistosoma mansoni motor activity, egg laying and viability. Parasitology. 1998;116 (
738 Pt 4):319-25. Epub 1998/05/20. PubMed PMID: 9585934.
739 51. Chaudhuri G, Chaudhuri M, Pan A, Chang KP. Surface acid proteinase (gp63) of
740 Leishmania mexicana. A metalloenzyme capable of protecting liposome-encapsulated
741 proteins from phagolysosomal degradation by macrophages. J Biol Chem.
742 1989;264(13):7483-9. Epub 1989/05/05. PubMed PMID: 2708373.
743 52. Chen L, Zhang ZH, Watanabe T, Yamashita T, Kobayakawa T, Kaneko A, et al.
744 The involvement of neutrophils in the resistance to Leishmania major infection in

745 susceptible but not in resistant mice. Parasitol Int. 2005;54(2):109-18. Epub 2005/05/04.
746 doi: 10.1016/j.parint.2005.02.001. PubMed PMID: 15866472.
747 53. Lima GM, Vallochi AL, Silva UR, Bevilacqua EM, Kiffer MM, Abrahamsohn IA.
748 The role of polymorphonuclear leukocytes in the resistance to cutaneous
749 Leishmaniasis. Immunol Lett. 1998;64(2-3):145-51. Epub 1998/12/31. PubMed PMID:
750 9870666.
751 54. McFarlane E, Perez C, Charmoy M, Allenbach C, Carter KC, Alexander J, et al.
752 Neutrophils contribute to development of a protective immune response during onset of
753 infection with Leishmania donovani. Infect Immun. 2008;76(2):532-41. Epub
754 2007/12/07. doi: 10.1128/IAI.01388-07. PubMed PMID: 18056477; PubMed Central
755 PMCID: PMCPMC2223441.
756 55. Novais FO, Santiago RC, Bafica A, Khouri R, Afonso L, Borges VM, et al.
757 Neutrophils and macrophages cooperate in host resistance against Leishmania
758 braziliensis infection. J Immunol. 2009;183(12):8088-98. Epub 2009/11/20. doi:
759 10.4049/jimmunol.0803720. PubMed PMID: 19923470.
760 56. Peters NC, Egen JG, Secundino N, Debrabant A, Kimblin N, Kamhawi S, et al. In
761 vivo imaging reveals an essential role for neutrophils in leishmaniasis transmitted by
762 sand flies. Science. 2008;321(5891):970-4. Epub 2008/08/16. doi:
763 10.1126/science.1159194. PubMed PMID: 18703742; PubMed Central PMCID:
764 PMCPMC2606057.
765 57. Rousseau D, Demartino S, Ferrua B, Michiels JF, Anjuere F, Fragaki K, et al. In
766 vivo involvement of polymorphonuclear neutrophils in Leishmania infantum infection.

767 BMC Microbiol. 2001;1:17. Epub 2001/10/10. PubMed PMID: 11591218; PubMed
768 Central PMCID: PMCPMC57739.
769 58. Smelt SC, Cotterell SE, Engwerda CR, Kaye PM. B cell-deficient mice are highly
770 resistant to Leishmania donovani infection, but develop neutrophil-mediated tissue
771 pathology. J Immunol. 2000;164(7):3681-8. Epub 2000/03/22. PubMed PMID:
772 10725726.
773 59. Tacchini-Cottier F, Zweifel C, Belkaid Y, Mukankundiye C, Vasei M, Launois P, et
774 al. An immunomodulatory function for neutrophils during the induction of a CD4+ Th2
775 response in BALB/c mice infected with Leishmania major. J Immunol.
776 2000;165(5):2628-36. Epub 2000/08/18. PubMed PMID: 10946291.
777 60. Thalhofer CJ, Chen Y, Sudan B, Love-Homan L, Wilson ME. Leukocytes infiltrate
778 the skin and draining lymph nodes in response to the protozoan Leishmania infantum
779 chagasi. Infect Immun. 2011;79(1):108-17. Epub 2010/10/13. doi: 10.1128/IAI.00338-
780 10. PubMed PMID: 20937764; PubMed Central PMCID: PMCPMC3019875.
781 61. Inbar E, Hughitt VK, Dillon LA, Ghosh K, El-Sayed NM, Sacks DL. The
782 Transcriptome of Leishmania major Developmental Stages in Their Natural Sand Fly
783 Vector. MBio. 2017;8(2). Epub 2017/04/06. doi: 10.1128/mBio.00029-17. PubMed
784 PMID: 28377524; PubMed Central PMCID: PMCPMC5380837.
785 62. Sacks D, Noben-Trauth N. The immunology of susceptibility and resistance to
786 Leishmania major in mice. Nat Rev Immunol. 2002;2(11):845-58. Epub 2002/11/05. doi:
787 10.1038/nri933. PubMed PMID: 12415308.
788 63. Leifso K, Cohen-Freue G, Dogra N, Murray A, McMaster WR. Genomic and
789 proteomic expression analysis of Leishmania promastigote and amastigote life stages:

790 the Leishmania genome is constitutively expressed. Mol Biochem Parasitol.
791 2007;152(1):35-46. Epub 2006/12/26. doi: 10.1016/j.molbiopara.2006.11.009. PubMed
792 PMID: 17188763.
793 64. Cronemberger-Andrade A, Aragao-Franca L, de Araujo CF, Rocha VJ, Borges-
794 Silva Mda C, Figueira CP, et al. Extracellular vesicles from Leishmania-infected
795 macrophages confer an anti-infection cytokine-production profile to naive macrophages.
796 PLoS Negl Trop Dis. 2014;8(9):e3161. Epub 2014/09/19. doi:
797 10.1371/journal.pntd.0003161. PubMed PMID: 25232947; PubMed Central PMCID:
798 PMCPMC4169249.
799 65. Silverman JM, Clos J, Horakova E, Wang AY, Wiesgigl M, Kelly I, et al.
800 Leishmania exosomes modulate innate and adaptive immune responses through effects
801 on monocytes and dendritic cells. J Immunol. 2010;185(9):5011-22. Epub 2010/10/01.
802 doi: 10.4049/jimmunol.1000541. PubMed PMID: 20881185.
803 66. Roque AL, Jansen AM. Wild and synanthropic reservoirs of Leishmania species
804 in the Americas. Int J Parasitol Parasites Wildl. 2014;3(3):251-62. Epub 2014/11/27. doi:
805 10.1016/j.ijppaw.2014.08.004. PubMed PMID: 25426421; PubMed Central PMCID:
806 PMCPMC4241529.
807 67. Baguet A, Epler J, Wen KW, Bix M. A Leishmania major response locus
808 identified by interval-specific congenic mapping of a T helper type 2 cell bias-controlling
809 quantitative trait locus. J Exp Med. 2004;200(12):1605-12. Epub 2004/12/15. doi:
810 10.1084/jem.20040334. PubMed PMID: 15596523; PubMed Central PMCID:
811 PMCPMC2211989.

812 68. Yu CL, Summers RM, Li Y, Mohanty SK, Subramanian M, Pope RM. Rapid
813 identification and quantitative validation of a caffeine-degrading pathway in
814 Pseudomonas sp. CES. J Proteome Res. 2015;14(1):95-106. Epub 2014/10/29. doi:
815 10.1021/pr500751w. PubMed PMID: 25350919.
816 69. Waterhouse AM, Procter JB, Martin DM, Clamp M, Barton GJ. Jalview Version 2-
817 -a multiple sequence alignment editor and analysis workbench. Bioinformatics.
818 2009;25(9):1189-91. Epub 2009/01/20. doi: 10.1093/bioinformatics/btp033. PubMed
819 PMID: 19151095; PubMed Central PMCID: PMCPMC2672624.

820
821
822

823 **Figure legends**
824
825

826 **Figure 1: *L. major* diminishes LPS-induced CXCL1 release by BMDMs.** (A) BMDMs
827 were treated with LPS (20 ng/ml) in the presence or absence of *L. major* (20 MOI) for 48h
828 and cell culture supernatants were analyzed for the indicated cytokines. (B) BMDMs were
829 treated with PBS or *L. major* (20 MOI) for 6h. Then, the cells were washed to remove
830 extracellular *L. major* and stimulated with LPS for next 42h and cell culture supernatants
831 were subjected to cytokines analysis as in (A). Data are representative of at least three
832 independent experiments. Results are represented as mean ± SEM. ***P<0.001.

833

834 **Figure 2: *L. major* inhibits CXCL1 detection in a cell free system.** (A) Conditioned
835 supernatants from 24h LPS (20 ng/ml)-stimulated BMDMs were treated with or without *L.*
836 *major* for 24h and cytokines were analyzed by ELISA. (B) 24h LPS treated conditioned
837 media from BMDMs were treated with or without *L. major*, *L. major* lysate (*Lm* lysate), or
838 *L. major* culture supernatant (*Lm* sup) for 24h and cytokines were measured as in (A).
839 Data are representative of at least three independent experiments. Results are
840 represented as mean ± SEM. ****P<0.0001.

841

842 **Figure 3: Selective inhibitory activity of *L. major* on recombinant murine CXCL1** (A)
843 Sequence alignment of recombinant murine (rm) and recombinant human (rh) CXCL1,
844 CXCL2, and CXCL8. (B) Rm-CXCL1, (C) rh-CXCL1, (D) rm-CXCL2, (E) rh-CXCL2, (F)
845 rh-CXCL8, and (G) rm-TNF were incubated with or without *Lm* sup for indicated time-
846 points and ELISA was performed to quantify the mentioned cytokine/chemokines. (H)

847 Rm-CXCL1 was incubated with or without *Lm* sup or *Lm* exosomes derived from indicated
848 strains of *L. major* for 24h, and CXCL1 quantification was performed as in (G). Data are
849 representative of at least three independent experiments. Results are represented as
850 mean ± SEM. ****P<0.0001.
851
852 **Figure 4: Biological activity of *L. major*-treated CXCL1 is diminished** (A) Schematic
853 representation of experimental design. (B) Recombinant murine CXCL1 was incubated
854 with *Lm* lysate for 24h and CXCL1 levels was determined by ELISA. (C) BMDMs were
855 treated *Lm* lysate, rm-CXCL1, or *Lm* lysate + rm-CXCL1 from (B) for indicated time-points
856 and mRNA expression of pro-inflammatory genes were evaluated by qPCR. Data are
857 representative of at least three independent experiments.
858
859 **Figure 5: *L. major* cleaves CXCL1 at the C-terminal end.** (A) A silver-stained SDS-
860 PAGE demonstrate time-dependent cleavage of rm-CXCL1. Rm-CXCL1 were left alone
861 or treated with *Lm* lysate for the indicated time points. Rm-CXCL1 bands were enlarged
862 to show the cleavage products on right. (B) Indicated chemokines were treated with *Lm*
863 lysate for indicated time-points and subjected to SDS-PAGE followed by silver-staining.
864 (C) Hypothesized *L. major* cleavage site on rm-CXCL1 based on the observed cleaved
865 rm-CXCL1 bands in (A and B). Arrow denotes possible cleavage site on CXCL1 (D)
866 Identification of CXCL1 cleavage site by Mass Spectrometry analysis (raw data presented
867 in Supplemental Fig. 4). Arrow represents cleavage site on rm-CXCL1 targeted by *L.*
868 *major*. Data in A and B are representative of at least three independent experiments.
869

870 **Figure 6: *L. major* metalloprotease cleaves CXCL1.** (A) Recombinant CXCL1 was
871 incubated with or without *Lm* sup containing (B) Roche cOmplete protease inhibitor, or
872 (C) Sigma P8340 protease inhibitor for indicated time-points and subjected to CXCL1
873 quantification using ELISA. (D) Recombinant CXCL1 was treated with *Lm* sup in th
874 presence of (E) EDTA or (F) 1,10-Phenanthroline for indicated time-points and CXCL1
875 degradation determined by ELISA. (G) Recombinant CXCL1 was treated with *Lm* sup in
876 the presence of 1,10-Phenanthroline for indicated time-points and CXCL1 degradation
877 determined by silver staining. (H) *Lm* lysate was immunoprecipitated with GP63 antibody
878 and Western blot was carried out to evaluate the levels of GP63 protein. (I) The fractions
879 from (H) were incubated with rm-CXCL1 for indicated time-points and ELISA was
880 performed to quantify the levels of CXCL1. Data are representative of at least three
881 independent experiments. Results are represented as mean ± SEM. ***P<0.001,
882 ****P<0.0001.
883
884
885 **Figure 7: Synthetic peptide spanning rm-CXCL1 cleavage site inhibits *L. major*-**
886 **mediated CXCL1 degradation.** (A) Schematic of synthetic peptide generation.
887 Alignment of full length murine CXCL1 with mature murine CXCL1 demonstrating the
888 schematic for generation of peptide#1, peptide#2 and blocking peptide. Peptide#1 and
889 peptide#2 were generated from the N-terminal region of full length murine CXCL1.
890 Blocking peptide spanning the *L. major* cleavage site on murine CXCL1 were generated.
891 *Lm* lysate-mediated degradation of rm-CXCL1 in the presence of (B) Activity of synthetic
892 peptides from (A) in inhibiting L. major-mediated degradation of rm-CXCL1. (C) Model of

893 *L. major* metalloprotease function on CXCL1 during infection. Data are representative of
894 at least three independent experiments. Results are represented as mean ± SEM.
895 ****P<0.0001.

896 **Supplemental Figure 1: CXCL1, IL-6, and TNF secreted by LPS-activated BMDMs**
897 **are stable in cell culture conditions.** Conditioned supernatants from 24h LPS (20
898 ng/ml) stimulated BMDMs were collected and further cultured for 0, 24, or 48h and stability
899 of CXCL1, IL-6 and TNF in the culture were determined by ELISA. Data are representative
900 of at least three independent experiments. Results are represented as mean ± SEM.
901

902 **Supplemental Figure 2: Heat inactivation of *Lm* lysate or *Lm* sup rescues CXCL1**
903 **detection.** (A) Experimental Design. (B) Conditioned supernatants from 24h LPS (20
904 ng/ml) stimulated BMDMs were collected and subjected to 24h treatment with control or
905 boiled (20 min at 100ºC) *Lm* lysate or *Lm* sup. Levels of CXCL1, IL-6 and TNF were
906 determined by ELISA. Results are represented as mean ± SEM. ****P<0.0001.
907

908 **Supplemental Figure 3: *L. major* reduces rm-CXCL1 levels in culture.** Rm-CXCL1
909 were left alone or treated with *Lm* sup (control or boiled) for up to 48 hours in culture. The
910 quantity of rm-CXCL1 in the culture at 0, 24 and 48 h were determined by ELISA. Data
911 are representative of at least three independent experiments. Results are represented as
912 mean ± SEM.
913

914 **Supplemental Figure 4:** Acute time course of *L. major*-induced CXCL1 cleavage. Rm-
915 CXCL1 were left alone or treated with *Lm* lysate for acute time points as indicated to

916 determine the precise time course of rm-CXCL1 cleavage. Silver staining was used to
917 visualize rm-CXCL1. Data are representative of at least three independent experiments.
918
919 **Supplemental Figure 5: Identification of CXCL1 cleavage site and cleaved products.**
920 (A) A silver-stained SDS-PAGE showing cleavage of full length (BAND 1) and cleaved
921 rm-CXCL1 (BAND 2). (B) Mass spectrometry analysis of BAND 1 (full length CXCL1) and
922 tryptic peptide coverage analysis confirm a full length rm-CXCL1. (C) Mass spectrometry
923 analysis of BAND 2 (cleaved CXCL1) and tryptic peptide coverage analysis confirm a C-
924 terminal end cleavage after K65 residue.
925
926 **Supplemental Figure 6: Proteolytic activity of *L. major* on CXCL1 is not prevented**
927 **by Roche cOmplete Inhibitor or Marimastat** (A) Conditioned supernatants from 24h
928 LPS (20 ng/ml)-stimulated BMDMs were collected and treated with *Lm* sup in the
929 presence or absence of Roche cOmplete protease inhibitor. Levels of CXCL1, IL-6 and
930 TNF were determined by ELISA. (B) Rm-CXCL1 was treated with *Lm* sup in the presence
931 or absence of Marimastat (10μM) for indicated time-points and ELISA was performed to
932 evaluate the levels of CXCL1. Data are representative of at least three independent
933 experiments. Results are represented as mean ± SEM. ***$P<0.001$, ****$P<0.0001$.
934

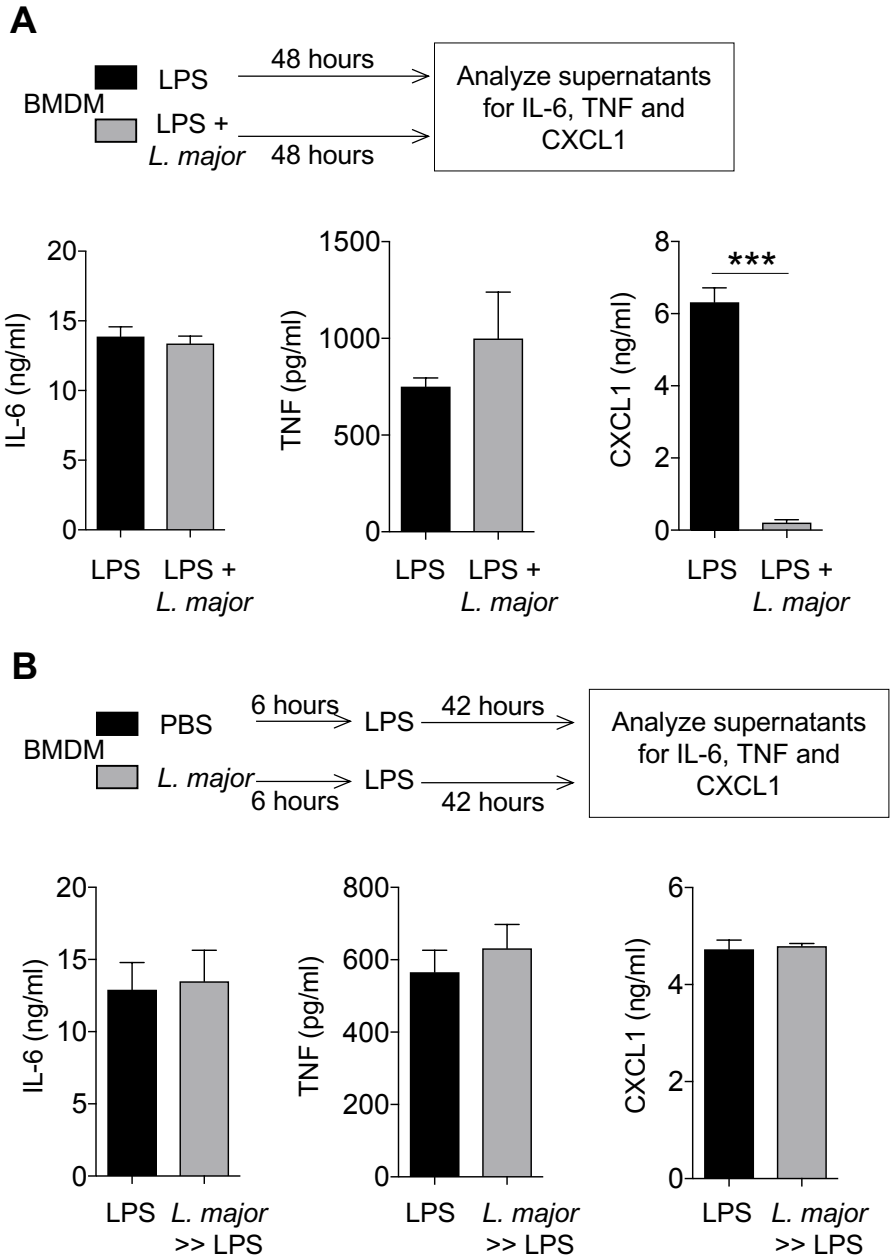
A
BMDM
LPS
LPS +
L. major
48 hours
48 hours
Analyze supernatants for IL-6, TNF and CXCL1
IL-6 (ng/ml)
TNF (pg/ml)
CXCL1 (ng/ml)
***
LPS
LPS + L. major
B
BMDM
PBS
L. major
6 hours
6 hours
LPS
LPS
42 hours
42 hours
Analyze supernatants for IL-6, TNF and CXCL1
IL-6 (ng/ml)
TNF (pg/ml)
CXCL1 (ng/ml)
LPS
L. major >> LPS

Figure 1

A

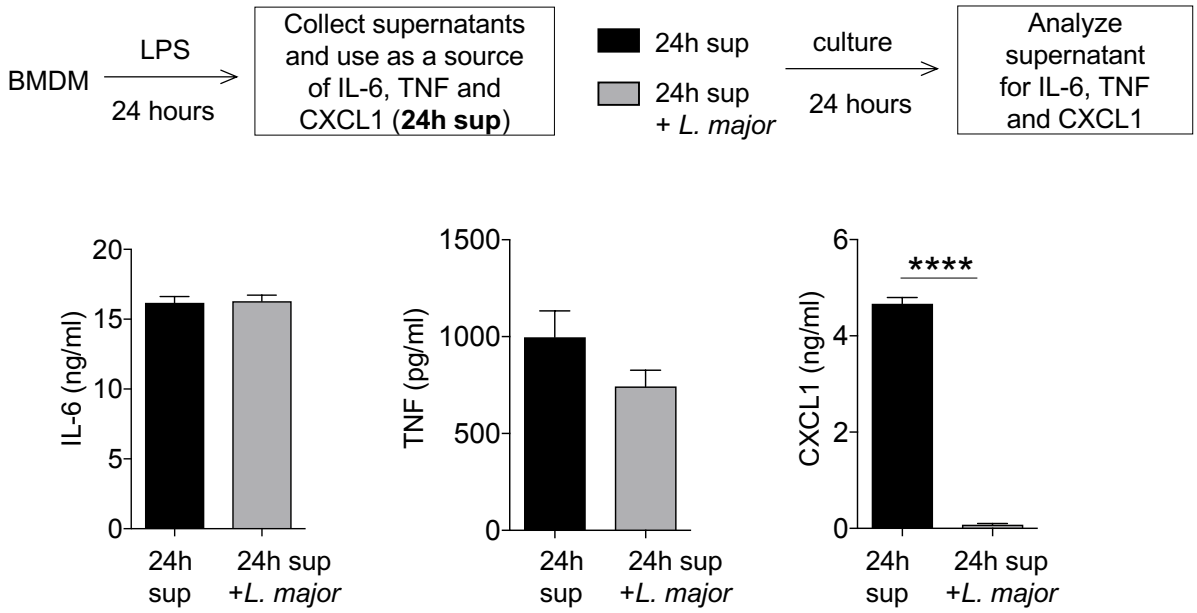
BMDM
LPS
24 hours
Collect supernatants and use as a source of IL-6, TNF and CXCL1 (**24h sup**)
24h sup
24h sup + *L. major*
culture
24 hours
Analyze supernatant for IL-6, TNF and CXCL1
IL-6 (ng/ml)
TNF (pg/ml)
CXCL1 (ng/ml)
****
24h sup
24h sup +*L. major*

B

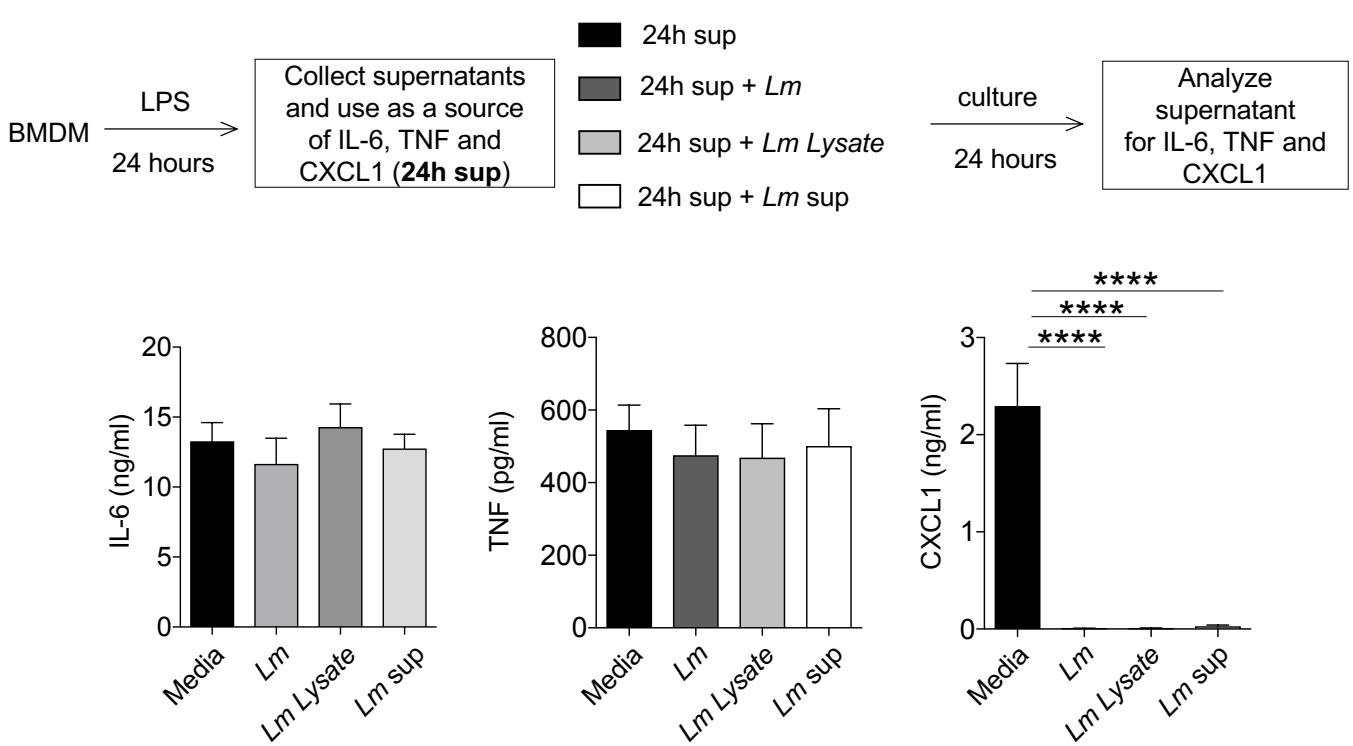
BMDM
LPS
24 hours
Collect supernatants and use as a source of IL-6, TNF and CXCL1 (**24h sup**)
24h sup
24h sup + *Lm*
24h sup + *Lm Lysate*
24h sup + *Lm* sup
culture
24 hours
Analyze supernatant for IL-6, TNF and CXCL1
IL-6 (ng/ml)
TNF (pg/ml)
CXCL1 (ng/ml)
****
Media
Lm
Lm Lysate
Lm sup

Figure 2

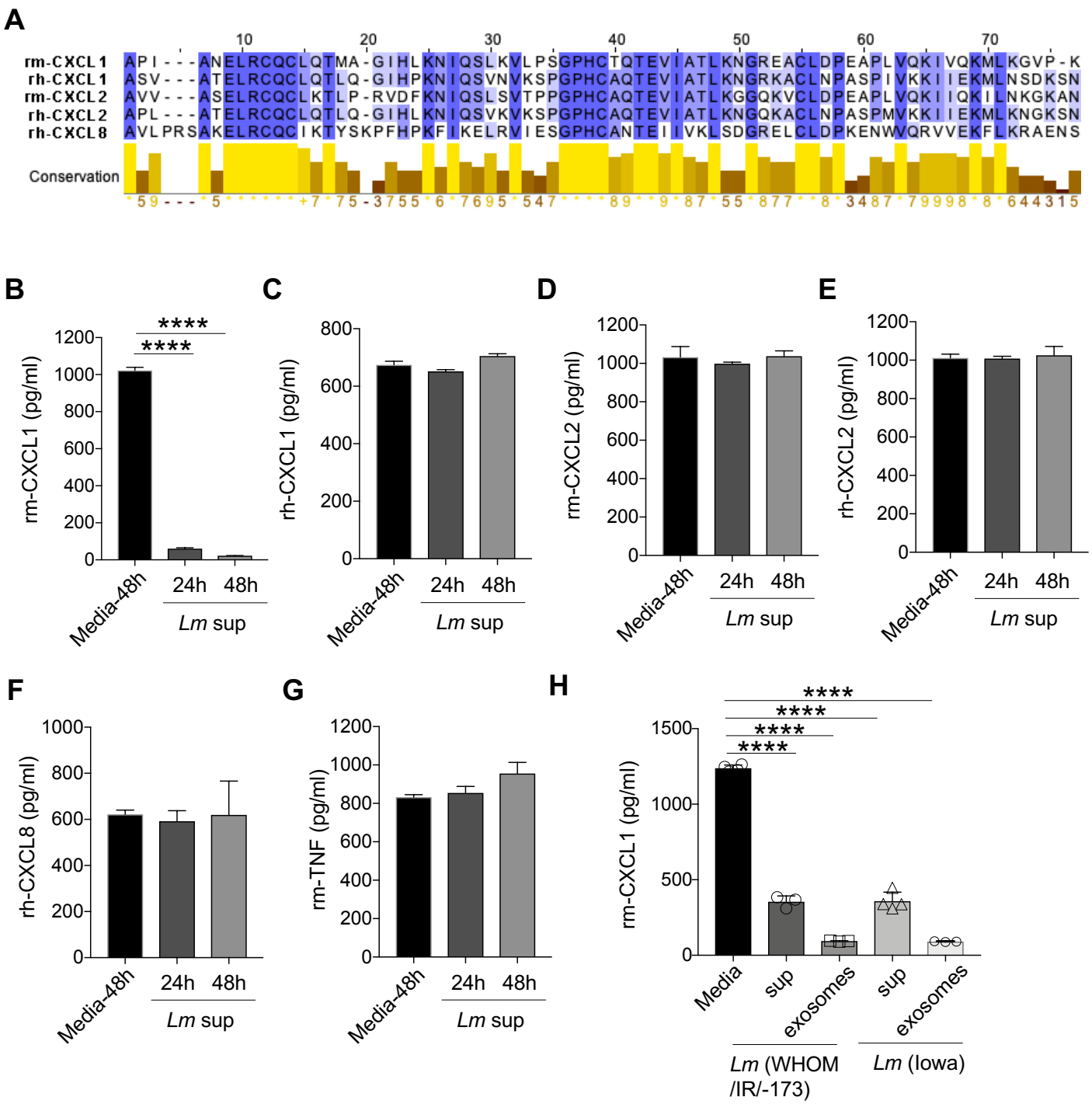
A
rm-CXCL1
rh-CXCL1
rm-CXCL2
rh-CXCL2
rh-CXCL8
Conservation
B
rm-CXCL1 (pg/ml)
****
****
Media-48h
24h
48h
Lm sup
C
rh-CXCL1 (pg/ml)
D
rm-CXCL2 (pg/ml)
E
rh-CXCL2 (pg/ml)
F
rh-CXCL8 (pg/ml)
G
rm-TNF (pg/ml)
H
rm-CXCL1 (pg/ml)
Media
sup
exosomes
Lm (WHOM /IR/-173)
Lm (Iowa)

Figure 3

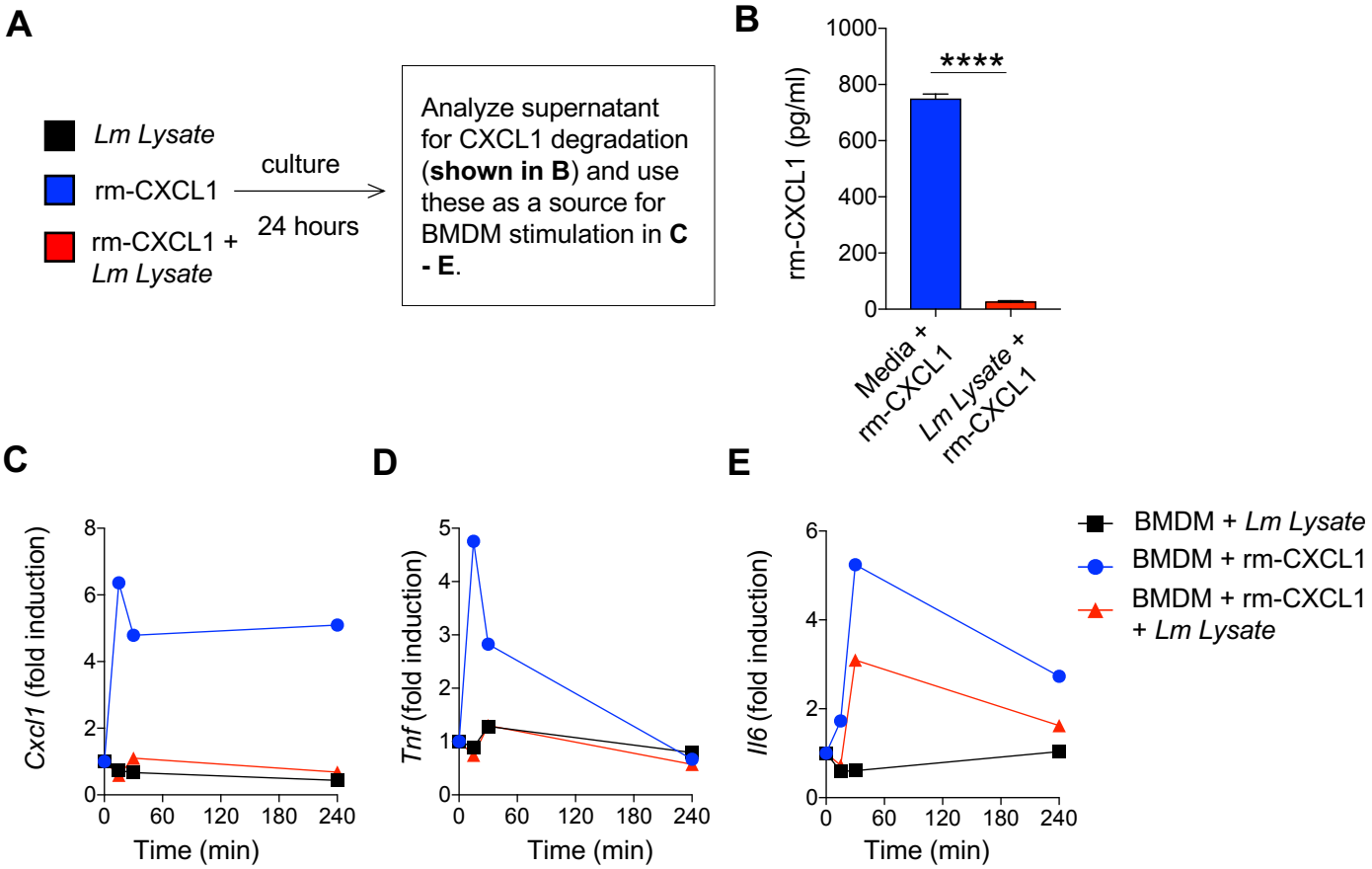
A
Lm Lysate
rm-CXCL1
rm-CXCL1 + Lm Lysate
culture
24 hours
Analyze supernatant for CXCL1 degradation (shown in B) and use these as a source for BMDM stimulation in C - E.
B
rm-CXCL1 (pg/ml)
1000
800
600
400
200
0
****
Media + rm-CXCL1
Lm Lysate + rm-CXCL1
C
Cxcl1 (fold induction)
Time (min)
D
Tnf (fold induction)
Time (min)
E
Il6 (fold induction)
Time (min)
BMDM + Lm Lysate
BMDM + rm-CXCL1
BMDM + rm-CXCL1 + Lm Lysate

Figure 4

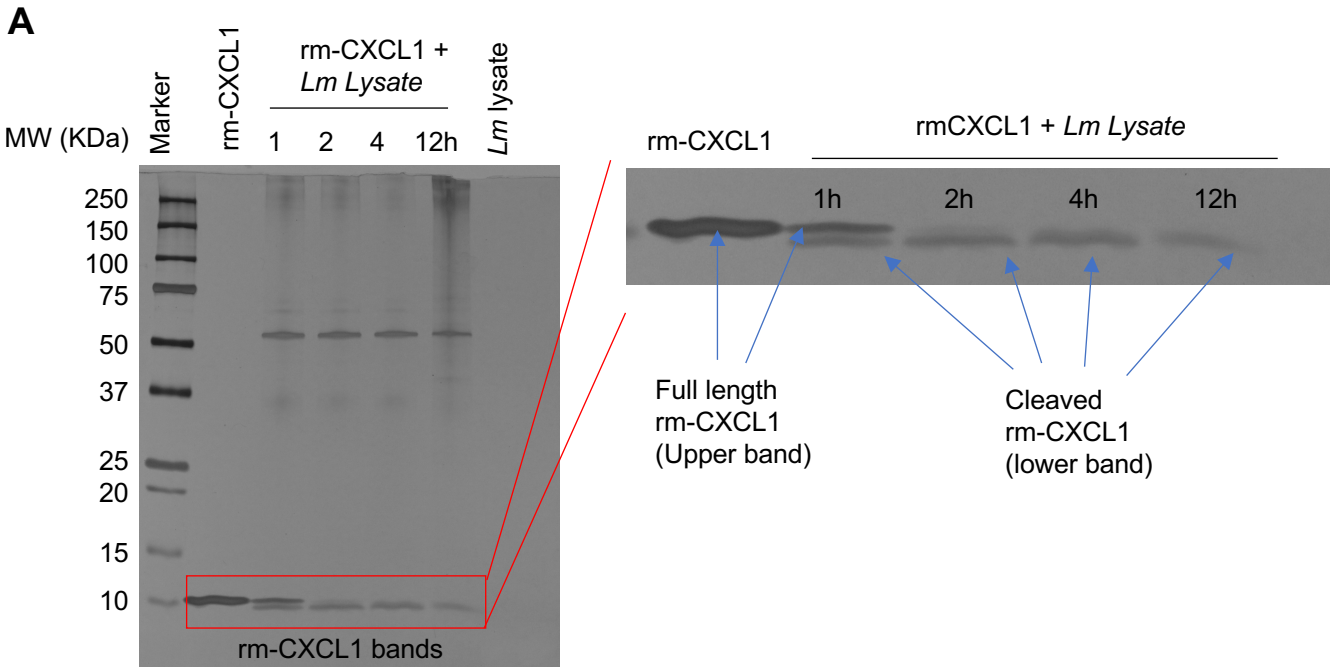
A
MW (KDa)
Marker
rm-CXCL1
rm-CXCL1 +
Lm Lysate
1 2 4 12h
Lm lysate
250
150
100
75
50
37
25
20
15
10
rm-CXCL1 bands
rm-CXCL1
rmCXCL1 + Lm Lysate
1h 2h 4h 12h
Full length
rm-CXCL1
(Upper band)
Cleaved
rm-CXCL1
(lower band)

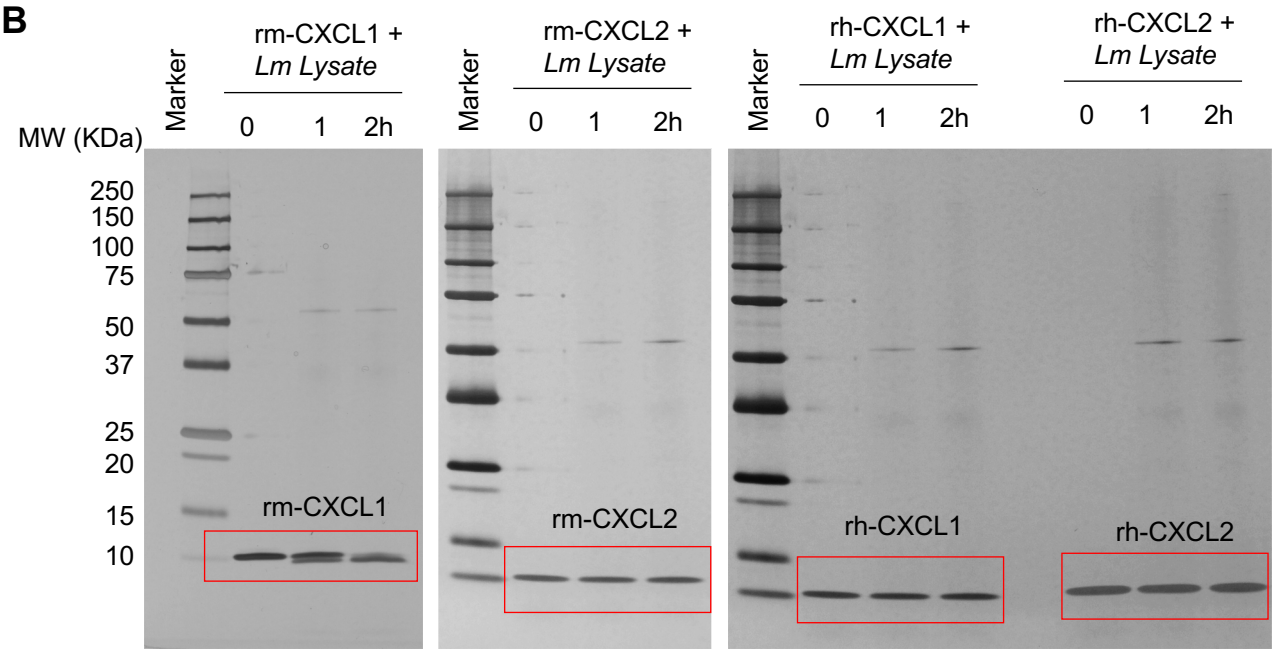
B
MW (KDa)
Marker
rm-CXCL1 +
Lm Lysate
0 1 2h
rm-CXCL2 +
Lm Lysate
0 1 2h
rh-CXCL1 +
Lm Lysate
0 1 2h
rh-CXCL2 +
Lm Lysate
0 1 2h
250
150
100
75
50
37
25
20
15
10
rm-CXCL1
rm-CXCL2
rh-CXCL1
rh-CXCL2

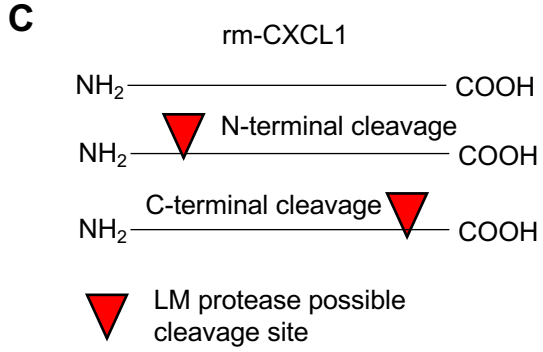
C
rm-CXCL1
NH2
COOH
N-terminal cleavage
NH2
COOH
C-terminal cleavage
NH2
COOH
LM protease possible
cleavage site

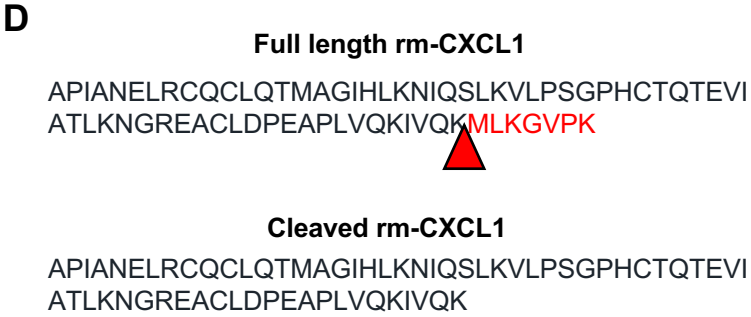
D
Full length rm-CXCL1
APIANELRCQCLQTMAGIHLKNIQSLKVLPSGPHCTQTEVI
ATLKNGREACLDPEAPLVQKIVQKMLKGVPK
Cleaved rm-CXCL1
APIANELRCQCLQTMAGIHLKNIQSLKVLPSGPHCTQTEVI
ATLKNGREACLDPEAPLVQKIVQK

Figure 5

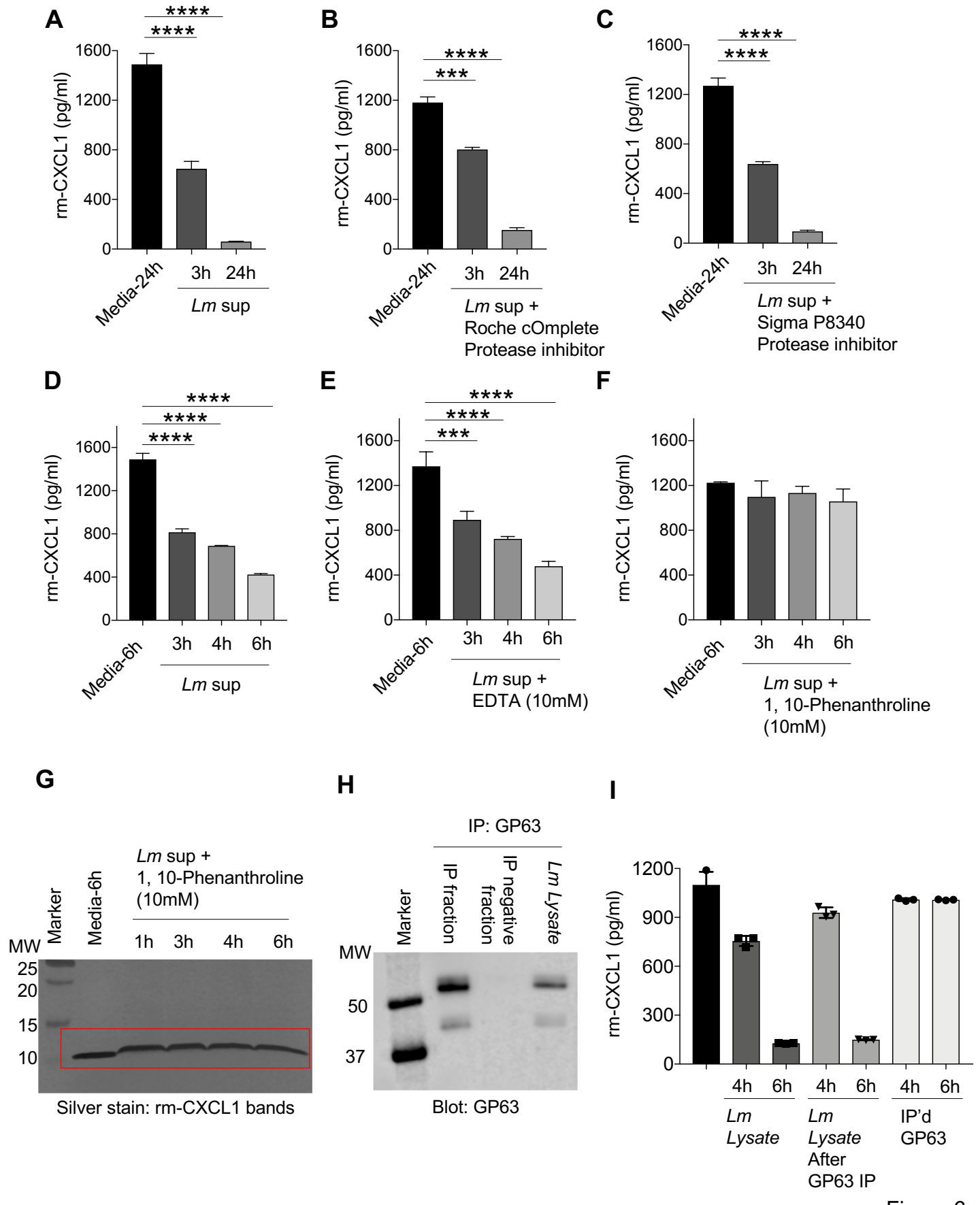
A
****
****
rm-CXCL1 (pg/ml)
1600
1200
800
400
0
Media-24h
3h
24h
Lm sup
B
****
***
Lm sup +
Roche cOmplete
Protease inhibitor
C
****
****
Lm sup +
Sigma P8340
Protease inhibitor
D
****
****
****
Media-6h
3h
4h
6h
Lm sup
E
****
****
***
Lm sup +
EDTA (10mM)
F
Lm sup +
1, 10-Phenanthroline
(10mM)
G
Lm sup +
1, 10-Phenanthroline
(10mM)
Marker
Media-6h
1h
3h
4h
6h
MW
25
20
15
10
Silver stain: rm-CXCL1 bands
H
IP: GP63
Marker
IP fraction
IP negative fraction
Lm Lysate
MW
50
37
Blot: GP63
I
1200
900
600
300
0
4h
6h
Lm Lysate
Lm Lysate After GP63 IP
IP'd GP63

Figure 6

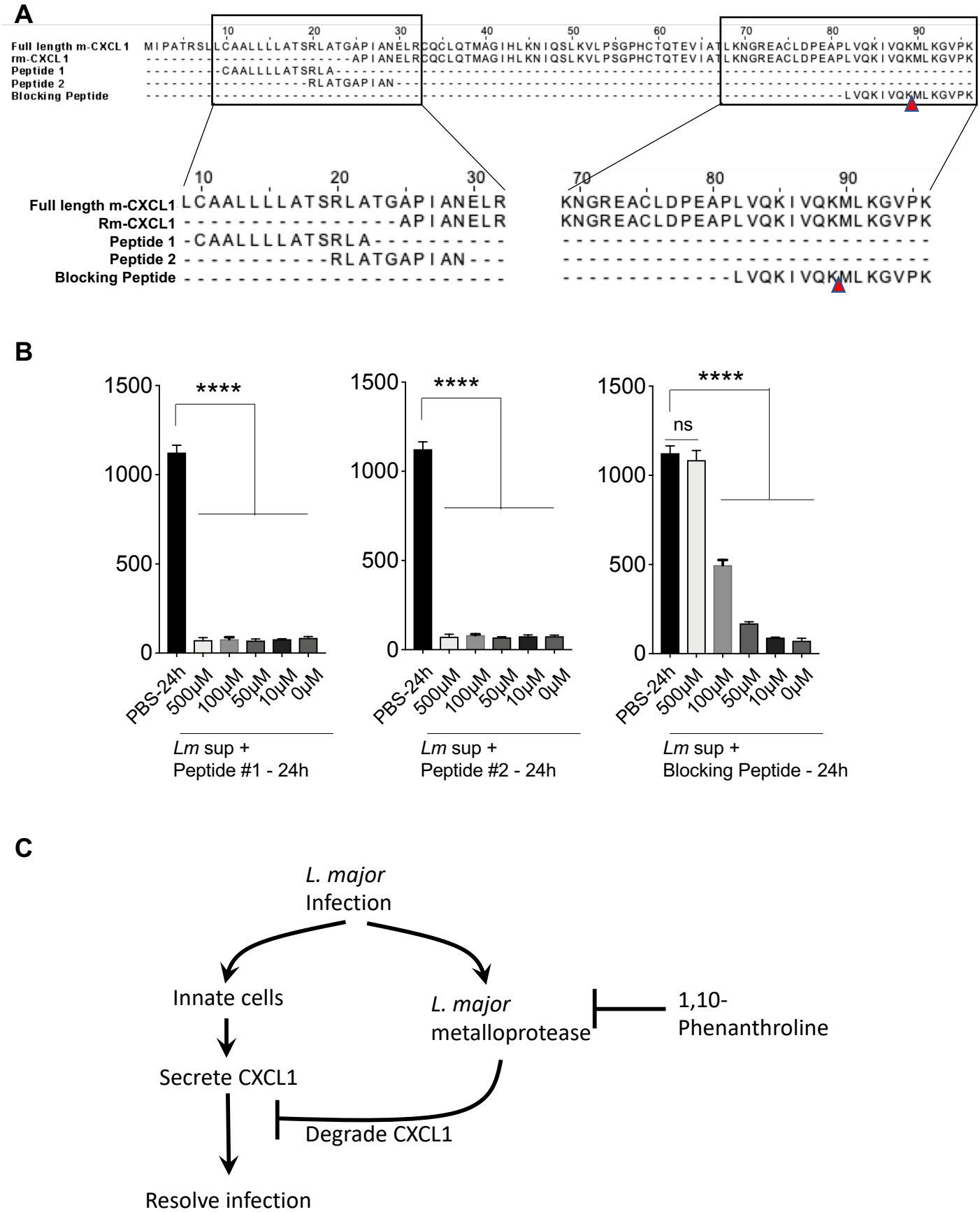
A
Full length m-CXCL1
rm-CXCL1
Peptide 1
Peptide 2
Blocking Peptide
B
****
ns
PBS-24h
500µM
100µM
50µM
10µM
0µM
Lm sup +
Peptide #1 - 24h
Peptide #2 - 24h
Blocking Peptide - 24h
C
L. major
Infection
Innate cells
Secrete CXCL1
Resolve infection
L. major
metalloprotease
1,10-
Phenanthroline
Degrade CXCL1

Figure 7

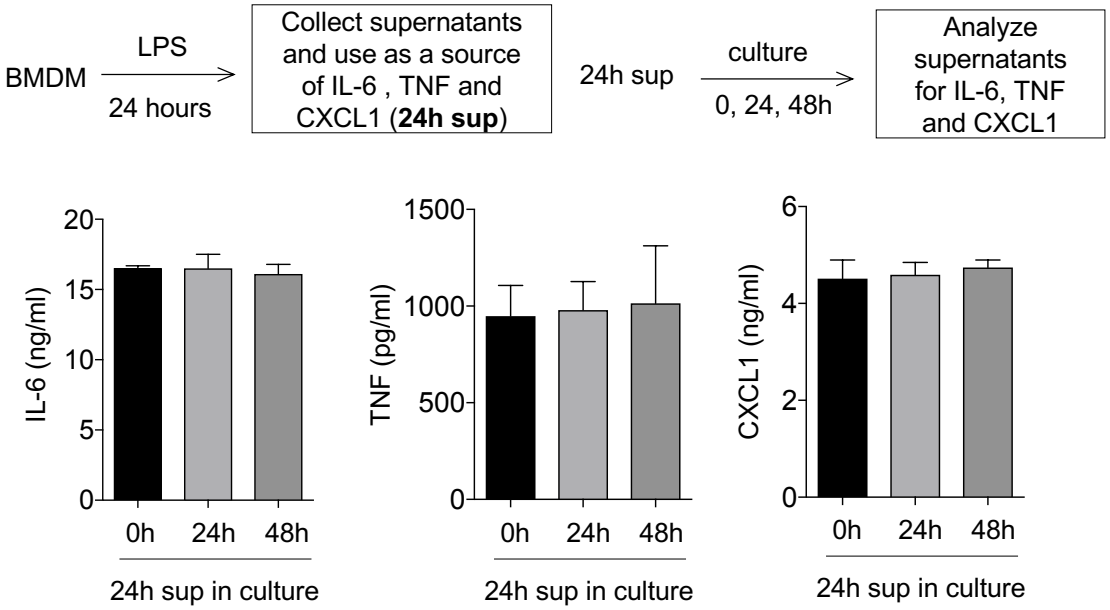

Supplemental Figure 1

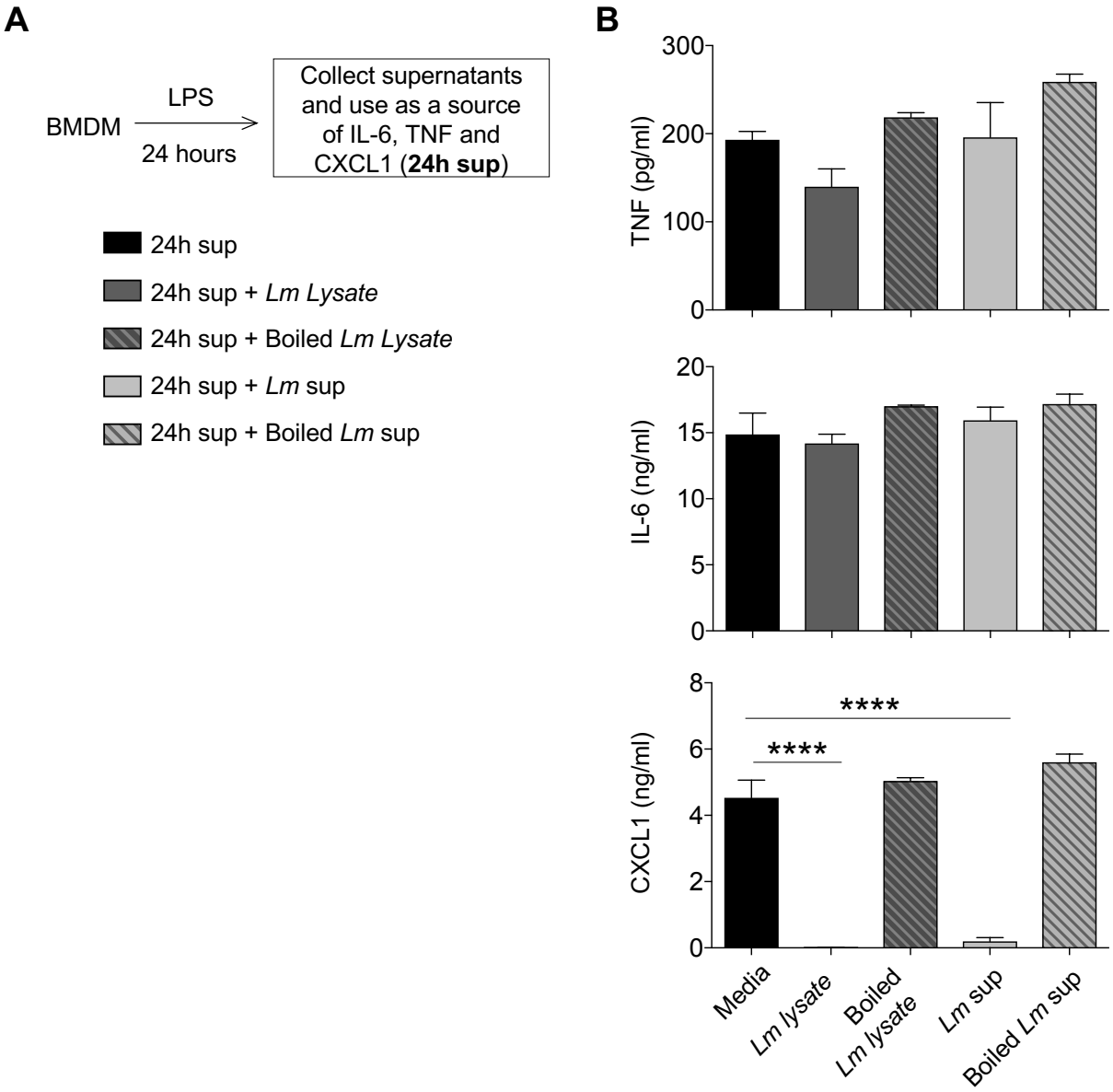

Supplemental Figure 2

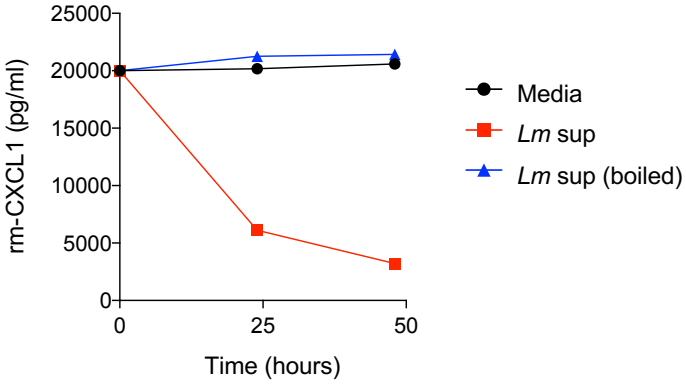

Supplemental Figure 3

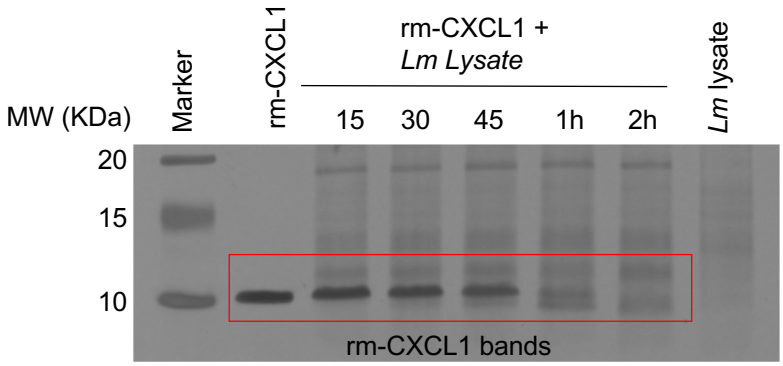

Supplemental Figure 4

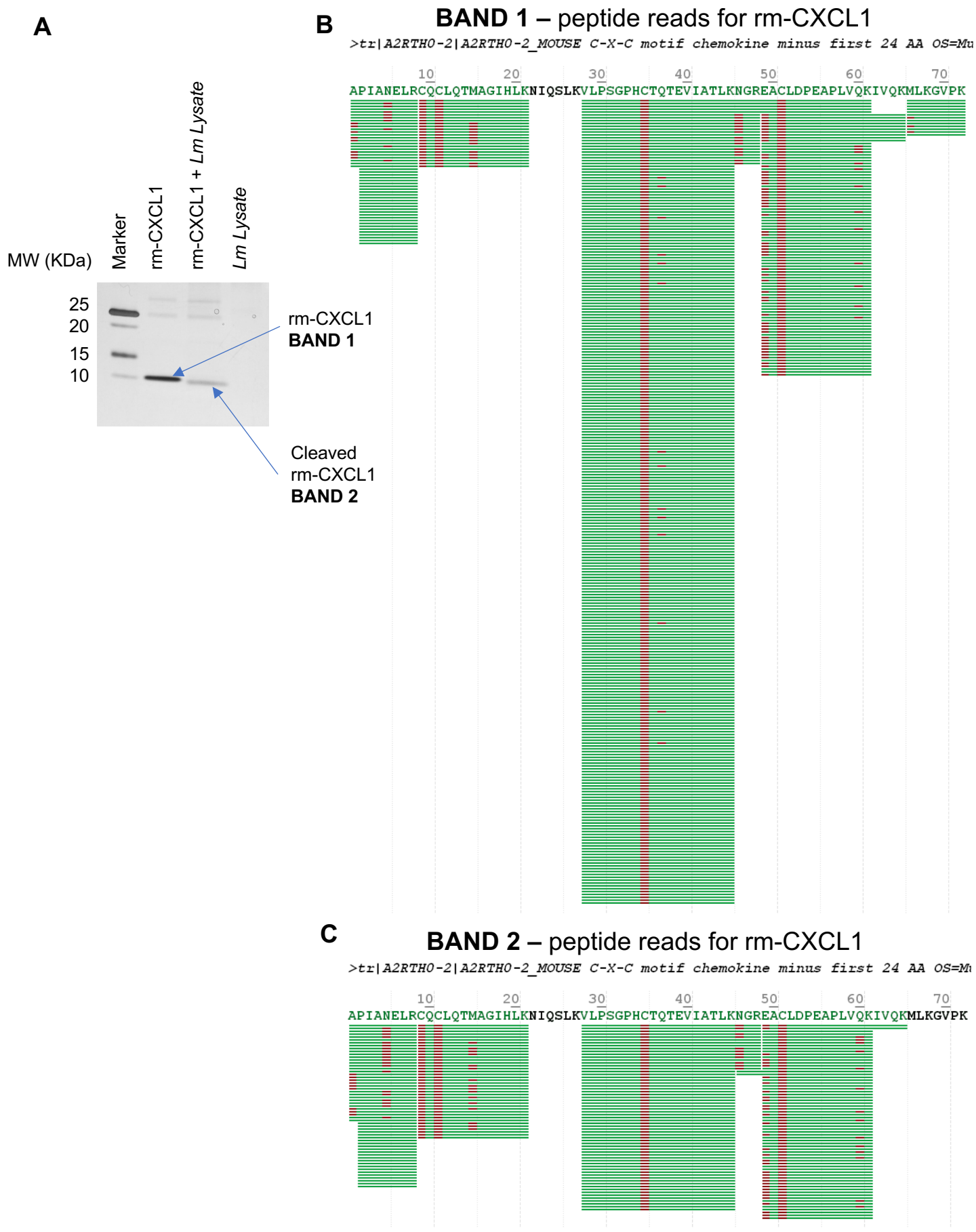

Supplemental Figure 5

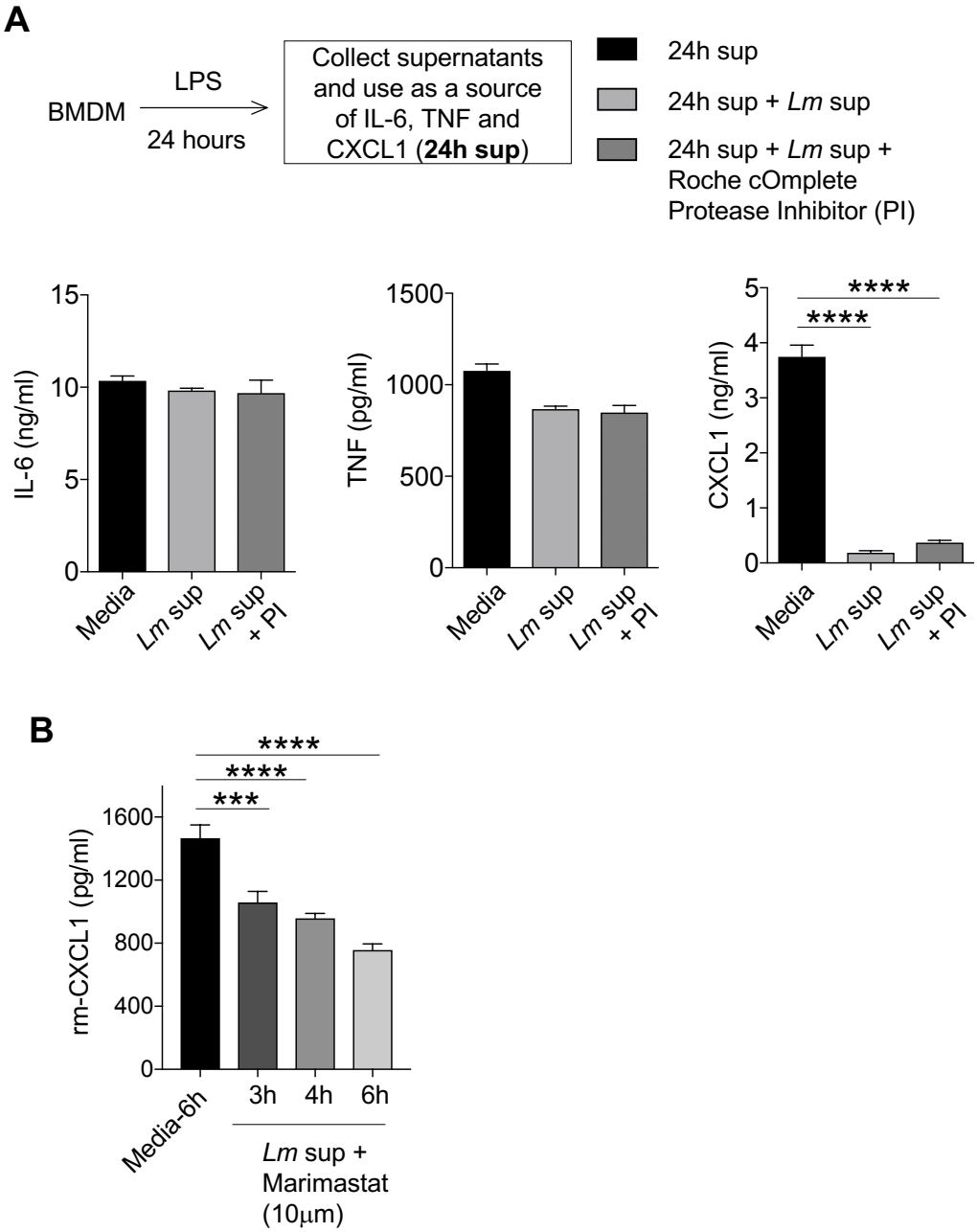

Supplemental Figure 6